Master's thesis

NTNU
Norwegian University of Science and Technology
Faculty of Medicine and Health Sciences
Department of Clinical and Molecular Medicine

Elisabeth Grønli

Exploring endoplasmic reticulum stress responses and senescence upon infection with respiratory syncytial virus

Master's thesis in Molecular Medicine
Supervisor: Marit Walbye Anthonsen
May 2024

NTNU
Norwegian University of
Science and Technology

Elisabeth Grønli

Exploring endoplasmic reticulum stress responses and senescence upon infection with respiratory syncytial virus

Master's thesis in Molecular Medicine
Supervisor: Marit Walbye Anthonsen
May 2024

Norwegian University of Science and Technology
Faculty of Medicine and Health Sciences
Department of Clinical and Molecular Medicine

NTNU
Norwegian University of
Science and Technology

Acknowledgements

This master thesis was conducted at the Department of Clinical and Molecular Medicine (IKOM), Faculty of Medicine and Health Sciences, Norwegian University of Science and Technology (NTNU) in Trondheim.

I would like to start by thanking my supervisor Marit W. Anthonsen for excellent guidance throughout this year. I have appreciated your support and feedback during this project. Your dedication to the field has been inspiring. I would also like to thank Kristin Rian for laboratory training and assistance in the lab.

A special thanks to my fellow students Synne-Lousie Trøen and Fredrik Simonsen Frossdal, for great moral support and informative discussions during this project. Finally, I would like to thank my family for believing in me and showing their support during this last year.

Elisabeth Grønli

May 2024, Trondheim

Abstract

Respiratory syncytial virus (RSV) is one of the most common causes of acute respiratory tract infection in infants and significantly impacts cellular mechanisms within host cells. Previous studies have revealed that RSV manipulates cellular stress mechanisms to enhance replication and survival. However, this activity can overload the endoplasmic reticulum (ER) in the host cell, disrupting normal function and inducing ER stress. ER stress activates the unfolded protein response (UPR), a cellular defense mechanism designed to restore ER function by halting protein translation, degrading misfolded proteins, and increasing the production of molecular chaperones.

This study examines the ER stress and UPR induced by RSV. Our findinds confirm that RSV induces ER stress and activates specific branches of the UPR, notably through the inositol requirering enzyme (IRE1)-X-box binding protein 1 (XBP1) and protein kinase R (PKR)-eukaryotic translation initiation factor 2α (eIF2α) axis. Our results also indicates that phosphorylation of eIF2α is mainly induced through PKR and not PERK. Moreover, we explore if cyclic GMP-AMP synthase (cGAS), and stimulator of interferon genes (STING) contributes to the activation of the PERK-eIF2α axis, revealing the cGAS-STING axis is not the most important axis for activation of PERK in RSV-infected WI-38 cells. We also revealed that RSV induced senescence, a cell cycle arrest inflammatory mechanism, in WI-38 cells, possibly due to prolonged UPR activation.

This study provides insight to the UPR and senescence induced by RSV infection in WI-38 lung fibroblasts. Additionally, this study gives insight into the importance of PKR-eIF2α axis in response to RSV infection. UPR and senescence mechanisms may be of relevance to understanding the fibrotic, inflammatory and aging effects that are observed in the lung after virus infection.

Sammendrag

Respiratorisk syncytialt-virus (RS-virus) er et av de vanligste årsakene til akutt respiratorisk infeksjon hos nyfødte og infeksjonen påvirker cellulære mekanismer i vertscellene. Tidligere studier har vist at RS-virus kan manipulere cellulære mekanismer for å fremme egen replikasjon og overlevelse, men dette kan føre til en overbelastning på endoplasmatisk retikulum (ER). Overbelastningen av ER vil forstyrre den normale funksjonen i cellen og føre til ER-stress. ER-stress aktiverer ufoldet proteinrespons signalvei (UPR), en cellulær forsvarsmekanisme som har i oppgave å rette opp i ER-stresset ved å bremse protein-translasjonen, degradere feilbrettede proteiner og øke produksjonen av molekylære chaperoner.

This study examines the ER stress and UPR induced by RSV. Our findinds confirm that RSV induces ER stress and activates specific branches of the UPR, notably through the inositol requirering enzyme (IRE1)-X-box binding protein 1 (XBP1) and protein kinase R (PKR)-eukaryotic translation initiation factor 2α (eIF2α) axis

Denne studien har gått ut på å undersøke ER-stress og UPR indusert av RS-virus. Våre funn har bekreftet at RSV gir ER-stress og aktivering av spesifikke UPR-grener, spesielt gjennom inositol requiering enzyme (IRE1)-X-box binding protein 1 (XBP1) og gjennom protein kinase R (PKR)-eukaryotisk translasjon initiasjon faktor 2α (eIF2α) signalveier. I tillegg har vi utforsket om syklisk GMP-AMP syntase (cGAS) og stimulator av interferon-gener (STING) bidrar til aktivering av PERK-eIF2α signalvei. Vi avslørte at cGAS-STING ikke er den viktigste signalveien for aktivering av PERK i RSV-infiserte WI-38 celler. Vi fant også ut at RSV induserer senescens i WI-38 celler, mest sannsynlig på grunn av langvarig aktivering av UPR.

Denne studien gir en innsikt i hvordan UPR og senescens blir indusert av RSV-infeksjon i WI-38 celler og i tillegg gir den en innsikt i viktigheten av PKR-eIF2α signalveien som en respons på RSV infeksjon i cellene.

Table of contents

Abbreviations

ATF4	Activation transcription factor 4
ATF6	Activation transcription factor 6
C/EBP	CCAAT-enhancer-binding protein
cDNA	Complementary DNA
cGAMP	Cyclic GMP-AMP
cGAS	Cyclic GMP-AMP synthase
CHOP	C/EBP homologous protein
CLR	C-type lectin receptors
DAMP	Damage-associated molecular pattern
DC	Dendritic cell
dsRNA	Double-stranded RNA
eIF2α	Eucaryotic translation initiation factor 2α
ER	Endoplasmic reticulum
ERAD	ER associated degradation
GADD34	Growth arrest and DNA damage 34
GAPDH	Glyceraldehyde 3-phosphate dehydrogenase
H3K9me3	Trimethylation of histone H3 lysine 9
IFN	Interferon
IFNAR	Interferon-α/β receptor
IKK	Inhibitor of NF-κB kinase
IL	Interleukin
IRE1	Inositol requiring enzyme 1
IRF3	Interferon regulatory factor 3
ISG	Interferon stimulated genes
JAK	Janus kinase
KD	Knockdown
mRNA	Messenger RNA
NF-κβ	Nuclear factor kappa-light-chain-enhancer of activated B cells
NK cells	Natural killer cells
PAMP	Pathogen-associated molecular pattern
PERK	Protein kinase R-like endoplasmic reticulum kinase

PKR	Protein kinase R
PRR	Pattern recognition receptor
RIG-I	Retinoic acid-inducible gene I
RLR	RIG-I like receptor
RSV	Respiratory syncytial virus
SASP	Senescence-associated secretory phenotype
siRNA	Small-interfering RNA
SNP	Single nucleotide polymorphism
STAT	Signal transducer and activator of transcription
STING	Stimulator of interferon genes
TBK1	TANK-binding Kinase 1
TLR	Toll-like receptor
UPR	Unfoled protein response
UV-RSV	UV-deactivated Respiratory syncytial virus
XBP1	X-box binding protein 1

1 Introduction

1.1 Viral respiratory infection

Virus is an infectious agent, depending on and exploiting the host cells machinery to propagate and reproduce viral genome and proteins (1). On the contrary, this intricate relationship offers the host cell mechanisms to defend itself against viral infection (2). The respiratory system encounters airborne microorganisms inevitably, while the majority are harmless components, a subset can initiate severe infection and disease (3). Infection in the respiratory tract is the leading cause of hospitalization in infants and young children and is the second cause of death of infants (4). Respiratory tract infections are caused by viral infections, with SARS-CoV-2 being a prominent example. By the end on 2021, the World Health Organization (WHO) reported approximately 287 million confirmed cases of SARS-CoV-2 globally, resulting in 5.4 million deaths (5). RNA virus like SARS-CoV-2 and respiratory syncytial virus (RSV) are the most predominant viral pathogens, together with influenza virus, parainfluenza virus, metapneumovirus and rhinovirus. (6, 7). Similar to influenza infections, RSV epidemics are often seasonal occurring. These infections usually have a peak occurring during winter months in temperate locations and around rain season in tropical, humid locations (8, 9).

1.2 Immune response to viral infection

The respiratory system is constantly in contact with airborne microbials. Airway epithelial cells functions as a passive barrier, protecting the body from airborne particles. Besides, airway epithelial cells have innate sensor functions, making them able to detect microbials (10). Alveolar macrophages and dendritic cells that sense and kill pathogens are examples of specialized immune cells in the lungs that are a part of the protective immune response and inflammatory response. (10, 11)

Airway epithelium is actively a part of the immune response by recognizing both pathogen-associated receptors (PAMPs) and damage-associated receptors (DAMPs). They achieve this through the expression pattern recognition receptors (PPRs) like Toll-like receptors (TLRs), RIG-I-like receptors (RLRs), C-type lectin receptors (CLRs) and inflammasome components. The

recognition of PAMPs by epithelial cells is a crucial part of the innate immune response against infection and activation of the adaptive immune system. (3, 12)

The immune system is a complex network of cells, chemicals and processes that function to protect humans from foreign antigens, viruses, cancers, and toxins. The innate immunity is referred to as the first line of defense against pathogens, responding rapidly to infections through non-specific mechanisms (12). It utilizes barriers like the skin and mucous membranes and consists of cells such as macrophages and natural killer (NK) cells, along with cytokines and interferons to rapidly contain and fight off invading pathogens (13). The adaptive immunity provides a targeted response to specific pathogens. It relies on more specialized cells like T-cells and B-cells to memorize and recognize pathogens for a more rapid and enhanced response during future encounters. (8, 13)

1.3 Interferon response to viral infection

Interferons are crucial components of the immune system, especially in response to viral infection. Interferons are released by infected host cells as a response to infection and can bind to receptors on neighboring cells, inducing cells to enhance their antiviral response (14). Interferons can also induce activation of genes encoding antiviral proteins to block viral replication (15). Additionally, interferons help activate macrophages and natural killer (NK) cells for more effective attack and killing of infected cells, preventing spread of infection. (15, 16)

There are three main types of interferons, Type I (IFN-α and IFN-β), Type II (IFN-γ) and type Type III (IFN-λ), each signaling through different receptors. (15) Type I IFNs are rapidly induced in response to viral infection and help establish an antiviral state in the body by activating genes that inhibit viral replication. Type II IFNs are important for their role in modulating the adaptive immune response and enhancing the ability of immune cells to eliminate pathogens. Type III IFNs are relevant in the respiratory tract and involved in controlling viral infection at mucosal surfaces without provoking excessive inflammation. (15, 17)

Production of type I interferons is often induced by PPRs that recognize PAMPs (18). IFN-α and -β binds to and signal through interferon-α/β receptors (IFNAR), which activates downstream cascades through Janus kinase (JAK) and signal transducer and activator of transcription 1

(STAT1) (19). The JAK-STAT pathway regulates the transcription and expression of interferon stimulated genes (ISGs), which induce an antiviral state in the cell and restricts viral replication in already infected cells. (15, 19)

1.4 Respiratory syncytial virus (RSV)

Respiratory syncytial virus (RSV) is one of the most common causes of acute respiratory tract infection in infants. The virus is cause for over 80% of lower respiratory tract infections in infants younger than one year (20). By the age of two, nearly all children are thought to have been exposed to RSV. Elderly individuals are the second major group at risk of severe infection. RSV have similar rates of mortality to influenza for elderly. (8)

RSV is an enveloped, spherical RNA virus in the Paramyxoviruses family and Pneumovirus genus (20). RSV is composed of two subgroups called A and B, and both subgroups causes annual epidemics. There is 13 RSV A genotypes and 20 RSV B genotypes (21). The envelope consists of three transmembrane proteins, the fusion glycoprotein (F), attachment glycoprotein (G) and the small hydrophobic protein (SH) (Figure 1). The G protein enables attachment of the virus to the host cell and the F protein initiates fusion of the host cell and the viral membranes. RSV and the host cell form a syncytium, a multinucleated cell, as a result from the membrane fusion (8, 21). The SH protein is thought to have a role in virulence, but its role is more unknown than F and G protein (8).

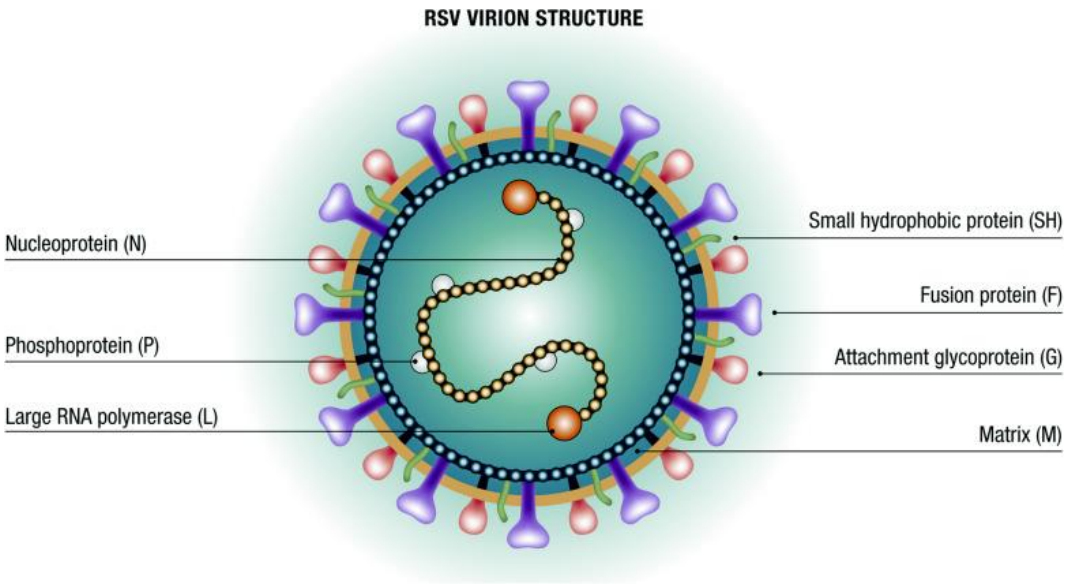

Figure 1: Structure of Respiratory suncytial virus (RSV) virion. The hydrophobic transmembrane surface attachment glycoprotein (G), Fusion protein (F) and small hydrophobic protein (SH) are all embedded in the viral protein and important during infection. Matrix proteins (M) lines the inside of the envelope. Viral RNA is encapsulated with nucleoproteins (N), Large protein (L), Phosphoprotein (P). (22)

The virus is mostly transmitted by close contact with saliva or mucus droplets and replicates in epithelial cells in nasopharynx and upper respiratory tract. Released virus particles can transfer to bronchioles or alveoli in the lower respiratory tract (4, 23). RSV has multiple mechanisms to avoid the immune system and limit host immunity. This allows the virus to replicate unhindered and leads to tissue damage and clinical symptoms of disease (8). In addition, RSV infection can cause an altered cytokine profile, which results in insufficient immune response and causes severe infection, contributing to bronchiolitis and pneumonia in young children and elderly. (24)

RSV can replicate quicky and rapidly generate single nucleotide polymorphisms (SNPs) and other mutations. This allows the virus to change its virulence and avoid antiviral agents and vaccines (25). There is currently no effective or safe vaccine against RSV or any RSV-specific therapeutics except from a couple of prophylactic drugs. These drugs are extremely expensive and is restricted to infants with considered high risk for severe RSV infection, such as infants born prematurely, with low body weight, underlying pulmonary conditions or that are immunocompromised. (26, 27)

1.5 Immune response to RSV

RSV infection causes the respiratory epithelial cells to secrete cytokines and chemokines (23). Secretion of cytokines and chemokines, together with upregulation of adhesion molecules causes a recruitment of immune cells like neutrophils, macrophages, T-cells and even some eosinophils to the site of infection (27).

Most of the damage caused by RSV infection is not from the virus itself, but from the immune response to the viral infection (23, 27). RSV target the epithelial cells, where it binds and enters through specific viral proteins, initiating the infection. This triggers the innate immune response and employs various PRRs to detect the virus. These receptors recognize PAMPs on RSV and this leads to activation of signaling pathways resulting in production of pro-inflammatory cytokines, including Type I IFNs, crucial for controlling the viral replication. (28)

RSV have strategies that employ the virus to evade and manipulate the immune response in the host cells. The G protein of RSV reduces the recruitment of innate immune cells by blunting the activity of chemokines and reduce the production of cytokines like IFN-b, IL-10 and IL-12 (29). RSV proteins NS1 and NS1 are important for RSV's regulation of interferon response and inhibition of IFN signaling (29). RSV can suppress Type III IFN production in lung epithelium, giving RSV an escape from the host antiviral response. (8, 29)

1.6 The cGAS-STING pathway

The cGAS-STING pathway is an essential component of the innate immune system and helps detect and respond to pathogens and damaged self-DNA. The pathway is crucial for controlling host defense, autoimmune disorder, autoinflammatory disorders and antitumor immunity (30). RSV is a single-stranded RNA virus that primarily infects epithelial cells in the respiratory tract. While cGAS-STING pathway is typically activated by DNA, there is emerging evidence suggesting that RNA viruses like RSV also can trigger this pathway indirectly. (31, 32)

The cGAS-STING pathway is activated through the PPR cyclic GMP-AMP-synthase (cGAS) detecting DNA from pathogens, chromosomes or mitochondria in the cytosol (Figure 2) (31, 33). As a response to foreign or damaged self-DNA, cGAS catalyzes the production of 2'3'-cyclic CMP-AMP (cGAMP). cGAMP binds to and activates the ER-associated protein stimulator of

interferon genes (STING). This complex leads to conformational change and autoactivation of STING. Subsequently, activated STING translocates to the Golgi apparatus. During the migration, the STING recruits TANK-binding kinase 1 (TBK1) and IkB-kinase (IKK). TBK1 phosphorylates the transcription factor interferon regulatory factor 3 (IRF3) and translocate to nucleus, while IKK activates NF-κB. In the nucleus, IRF3 works as a transcription factor to transcribe interferons and IFN-stimulated genes (ISGs). Activation of NF-κβ leads to production of additional inflammatory cytokines crucial for initiation of an effective antiviral immune response. (31, 33)

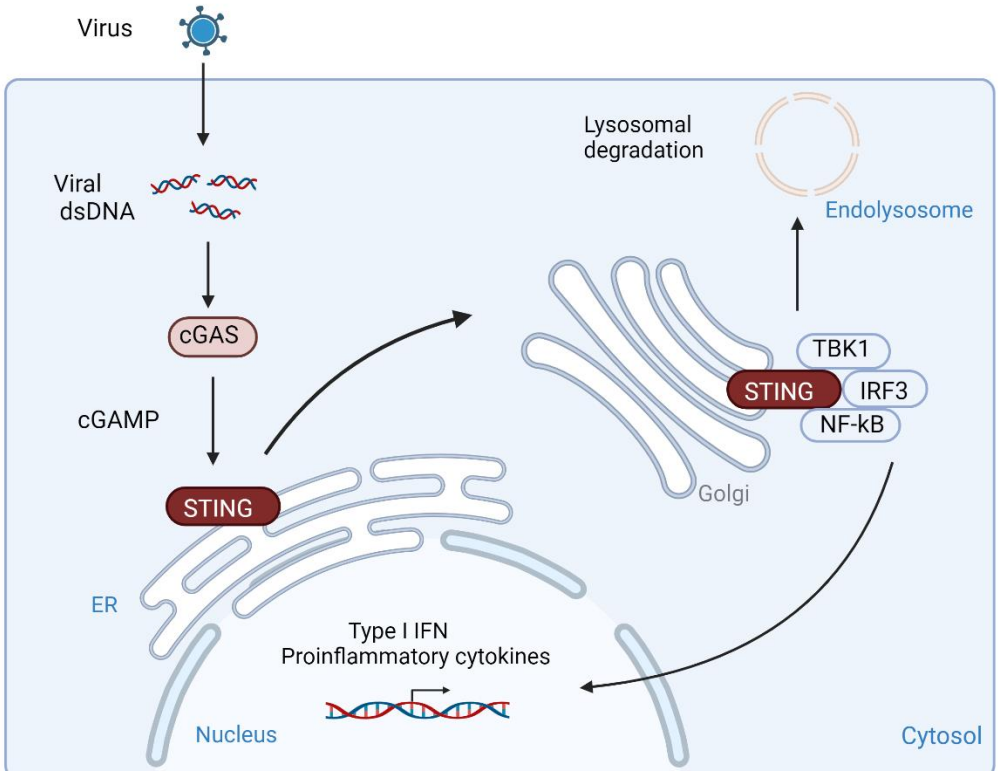

Figure 2: A simplified schematic of the canonical cGAS-STING pathway. Foreign or self-dsDNA is detected by cyclic GMP-AMP synthase (cGAS), and active cGAS generates 2'3'-cyclic GMP-AMP (cGAMP). cGAMP binds to stimulator of interferon genes (STING) located in the ER-membrane and induce conformational changes of STING. Upon conformational changes STING translocate from the ER to the Golgi apparatus or perinuclear compartments. TANK-binding kinase 1 (TBK1) is recruited to STING during translocation, leading to phosphorylation of STING and (interferon regulatory factor 3 (IRF3). IRF3 dimerizes and enters the nucleus to initiate type I interferon production and further IFN-signaling. Activation of STING also leads to NF-κβ activation. In the end, STING relocate to the lysosome, where it is degraded. Adapted from (34) and reacted with BioRender.com.

1.7 A non-canonical STING-PERK pathway

Zhang et al. identified a previously unknown function of STING in the ER: the regulation of mRNA cap dependent translation through STING-protein kinase R-like endoplasmic reticulum kinase (PERK)-eucaryotic translation initiation factor 2α (eIF2α) signaling pathway. The STING-PERK pathway is triggered when cGAS binds to and activates STING. Once activated, STING forms an interaction with the kinase domain PERK via its intracellular domain and activates PERK. The activated PERK phosphorylates eIF2α and leads to an inflammatory response where protein synthesis is regulated to help the cell handle stress caused by viral infection or other disturbances (Figure 3). The pathway can influence cellular processes, including autophagy, apoptosis, and inflammation. (30)

PERK is an ER transmembrane protein consisting of two domains: cytosolic kinase domain and a regulatory luminal domain (35). The regulatory luminal domain can sense ER stress and induce activation. Phosphorylated PERK can phosphorylate the alpha subunit of the eIF2. eIF2α forms a complex with eIF2β and suppresses the activity of eIF2β, which reduces the ER load by inhibition of peptide production (36). Phosphorylated eIF2α stimulates the translation of transcription factor ATF4. ATF4 induces expression of C/EBP homologous protein (CHOP), which induces expression of growth arrest and DNA damage 34 (GADD34) (36). CHOP is a transcription factor that promotes apoptosis during prolonged ER stress conditions. CHOP regulates the expression of genes promoting cell death and downregulates genes involved in cell survival. (35-37)

The pathway is crucial for managing ER stress induced by viral infection or other pathological conditions. By limiting protein synthesis, the pathway helps maintain cellular homeostasis and prevent the accumulation of unfolded or misfolded proteins, which can be toxic to the cell. Modulation of this pathway can have therapeutic effects, especially in disease where ER stress and inappropriate immune activation are pathological features. This can be in certain neurodegenerative diseases and cancers. (38, 39)

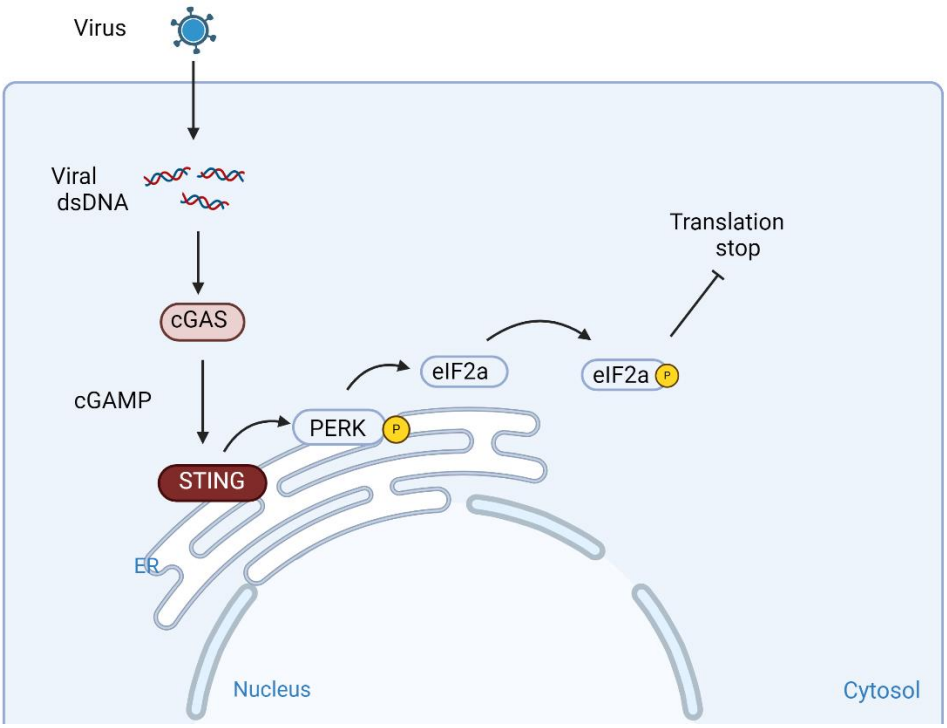

Figure 3: A simplified schematic of a non-canonical STING-PERK pathway. Foreign or self-dsDNA is detected by cyclic GMP-AMP synthase (cGAS), and active cGAS generates 2'3'-cyclic GMP-AMP (cGAMP). cGAMP binds to stimulator of interferon genes (STING) located in the ER-membrane and induce conformational changes of STING. STING binds to and phosphorylate PERK, which upon activation phosphorylate eIF2α. Phosphorylated eIF2α causes stop in translation. Adapted from (30, 40) and created with BioRender.com.

1.8 Endoplasmic reticulum (ER) stress and unfolded protein response (UPR)

The endoplasmic reticulum (ER) is a large organelle in the eukaryotic cell. One of the ERs tasks is to modify and fold proteins (36). Many viruses use the ER as a replication site, where they synthesize proteins, replicate genomes, and assemble virion. (41)

The ER is designed as a network of membrane structures divided into the nuclear envelope and the periphery ER, differentiated into sheets and tubules. The sheets are often referred to as rough ER and is characterized by their stubbed appearance due to the high density of ribosomes. Rough ER is a crucial site for protein folding and post-translational modifications. Tubules are smooth and highly curved. They host the calcium storage and lipid synthesis machinery of the ER. (42)

If the protein synthesis and folding in the ER is disrupted, it can result in an accumulation of misfolded or unfolded proteins in the ER lumen, referred to as ER stress. ER stress can cause activation of protein kinase R (PKR) which is a vital component of the cellular antiviral response

and is a kinase able to phosphorylate eIF2α (43). PKR's antiviral mechanism involves binding to double-stranded RNA (dsRNA) produced during viral replication, triggering a conformational change that leads to autophosphorylation and activation. Once active, PKR inhibits viral replication by phosphorylating eIF2α, thus blocking protein synthesis. (44)

ER stress can also result in activation of the unfolded protein response (UPR) (45). The UPR's main tasks are to restore normal function in the ER by halting protein translation and activating signaling pathways that increase the production of molecular chaperones involved in protein folding. In addition, the UPR enhance degradation of misfolded proteins through a process known as ER-associated degradation (ERAD) to clear the misfolded proteins from the ER. Lastly, UPR initiate apoptosis if the ER stress is severe and prolonged, and the corrective actions fail to restore ER function. (36, 42) UPR is a three-branch system consisting of the transmembrane sensor proteins PERK, inositol-requiring enzyme 1 (IRE1) and activating transcription factor 6 (AT6) (Figure 4). These proteins are normally inactivated by being bound to BiP, which actively promotes protein folding. Accumulation of misfolded or unfolded proteins stimulates BiP to dissociate from the UPR proteins and activates them. PERK and IRE1 shift to oligomers and is activate through autophosphorylation. ATF 6 is cleaved in the Golgi apparatus and turns into its active form before entering the nucleus to promote activation of UPR genes. (36, 42)

PERK is a transmembrane protein, which is autophosphorylated at Thr-982. This phosphorylation activates the PERK-protein, enabling it to phosphorylate eIF2α at serine 51, which leads to the dampening of protein synthesis (44) (Figure 4). This results in reduced overall protein synthesis by inhibition of translation initiation, helping to alleviate ER stress. (45)

IRE1 encodes two IRE1 isoforms, IRE1α and IRE1β. IRE1α is widely expressed across various tissues, whereas IREβ is especially expressed in intestinal epithelial cells and airway mucous cells. During ER stress, dimerization of IRE1 leads to autophosphorylation of the kinase domains (46). This activation enables IRE1 to initiate several intracellular signaling pathways through its RNase activity and promote apoptosis (46, 47). Additionally, activated IRE1 initiate the non-conventional splicing of XBP1s mRNA, removing an intron to produce spliced XBP1 (XBP1s) (Figure 4). This splicing results in a frameshift that extends the protein to include a transactivation domain, distinguishing the spliced form XBP1s from the unspliced XBP1 (46).

The presence of the transactivated XBP1s not only enhances its transcriptional activity but also affects protein stability. (45, 46, 48)

ATF6 is a basic leucin zipper (bZIP) translocation factor consisting of the isoforms ATF6α and ATF6β, both widely expressed across different tissues (47). These isoforms vary in their transaction domain, affecting their transcriptional activity differently. Unlike PERK and IRE1, ATF6 acts both as a sensor and effector in the UPR. Under stress conditions, the release of BiP from ATF6 directs to the Glogi apparatus, where it is cleaved by two proteases (S1P and S2P), into an active 50 kDa fragment, ATF6p50 (46). Once cleaved, ATF6p50 moves to the nucleus and influences the transcription of UPR genes. ATF6p50 activates a specific set of transcriptional programs that enhance the ER's protein-folding capabilities and increases protein degradation through the ERAD pathway (Figure 4). Additionally, ATF6 stimulates the expression of several key transcription factors, including CHOP and XBP1, further integrating its role in managing ER stress. (45-47)

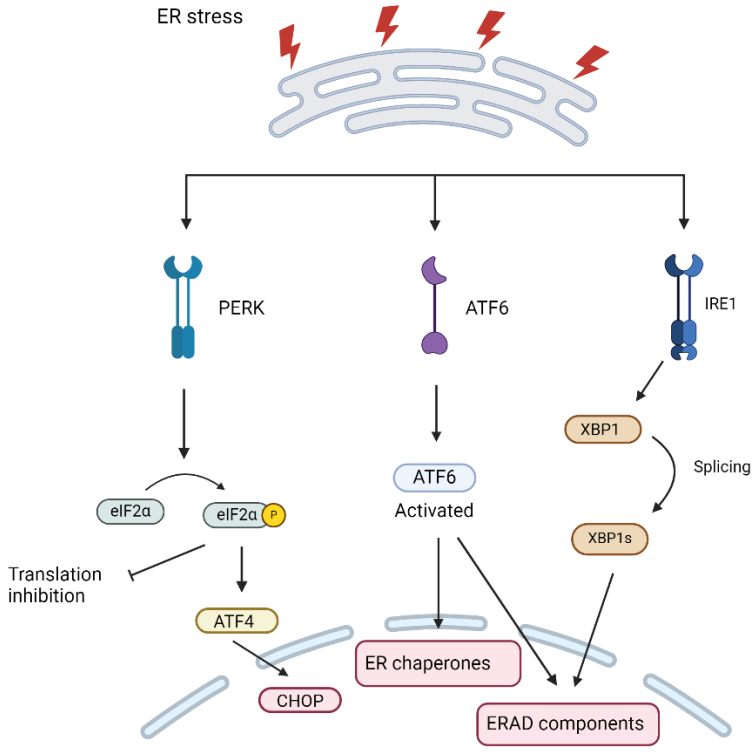

Figure 4: Unfolded protein response (UPR) pathways in the Endoplasmic Reticulum (ER) in a cell under stress from unfolded or misfolded proteins. There are three primary UPR sensors: Protein Kinase RNA-like Endoplasmic Reticulum Kinase (PERK), Activation transcription factor 6 (ATF6) and inositol requiring enzyme 1 (IRE1), each plays a distinct role in response to ER stress. PERK pathway: PERK phosphorylates eucaryotic initiation factor 2α /eIF2α), which increases activation transcription factor 4 (ATF4) translation and regulates genes involved in ER stress response. ATF6 Pathway: ATF6 translocates to the Golgi

apparatus where it is cleaved to form activation ATF6. Activated ATF6 enters the nucleus to enhance the transcription of UPR target genes including chaperones and components of the ER-associated degradation (ERAD) pathway. IRE1 Pathway: IRE1 is activated through autophosphorylation. It splices X-box binding protein 1 (XBP1) mRNA, creating spliced XBP1(s), an active transcription factor that induces genes improving protein folding capacity and components of ERAD, thereby promoting cell survival. Created with BioRender.com

1.9 Senescence

Cellular senescence is a state of stable, irreversible cell cycle arrest. It is a process where the cell permanently stops dividing and enter a state of permanent growth arrest, without undergoing cell death. Senescence is a natural part of aging of the cell and plays a critical role on various biological processes, including development, tissue repair and cancer prevention. (49)

Senescence can be triggered by several factors such as DNA damage, oxidative stress and telomere shortening. It serves as a protective mechanism to prevent propagation of damaged cells, reducing the risk of developing cancer (49). STING-associated vasculopathy with onset in infancy (SAVI) is a rare disease characterized by chronic, uncontrolled production of type I interferons, caused by a mutation in the STING protein. SAVI plays a crucial role in fibrosis development and the ongoing inflammatory state can accelerate the cellular aging process, leading to senescence (50, 51).

Senescent cells undergo significant changes in their function and morphology, including increases in size, changes in the gene expression and secretion of certain proteins that can affect the neighboring cells. This secretion is often referred to as the senescence-associated secretory phenotype (SASP) (49). SASP is characterized by secretion of pro-inflammatory cytokines and agents that modify the extracellular matrix. SASP has a crucial function across different biological contexts, including embryonic development, aging, responses to oncogenic and cancer therapy-induced stress and tissue damage repair (52). SASP is activated by senescent cells that can be triggered by the cGAS-STING pathway and NF-κβ and C/EBP signaling in response to DNA damage (52).

Senescent cells contain β-galactosidase. β-galactosidase is a lysosomal hydrolase which cleaves terminal β-d-galactosidase residues. The amount of lysosomes correlates with replicative age of the cell (53). Senescence-associated β-galactosidase (SA-β-gal) is a widely used biomarker for detection of cellular senescence. The SA-b-gal activity increases significantly in senescent cells,

compared to quiescent or proliferating cells. Almost all mammalian cells express lysosomal β-galactosidase activity at pH 4, but the enzyme can be used to detect senescent cells as pH 6. This unique feature can be used to distinguish senescent cells in tissue samples or culture. (54) Single-stranded and double-stranded DNA and RNA viruses can induce senescence in cells (52). RSV and measles promote cellular fusion, creating cellular stress that can lead to virus-induced senescence (55, 56).

Aim of study

The initial aim of this study was to explore the mechanisms of ER stress and unfolded protein response in RSV-infected lung fibroblast. Specifically, we sought to understand how RSV trigger the UPR following infection and to investigate the roles of PERK-eIF2α or PKR- eIF2α pathways in this process. Additionally, whether the cGAS-STING pathway contributes to activation of PERK-eIF2α or PKR- eIF2α axis was determined. Another key aspect of our research was to explore the effects of RSV infection on induction of senescence in WI-38 cells. By elucidating these mechanisms, this study intended to enhance our understanding of cellular response to UPR, focusing on how the host cell utilizes the UPR during RSV infection.

The following goals were pursued:

- Examine the ability of RSV to induce different unfolded protein response (UPR) branches in HEp-2 and WI-38.
- Examine if RSV stimulates activation of PERK and PKR during infection.
- Explore the effect of PERK and PKR on UPR in HEp-2 and WI-38 cells.
- Examine if cGAS and STING contributes to activation of PERK-eIF2α and PKR-eIF2α axis.
- Evaluate if RSV can induce senescence in WI-38 cells and the potential impact of UPR in this response.

2 Methodology

2.1 Cell cultivation

HEp-2 epithelial cells and WI-38 cells were utilized for this project. HEp-2 is a human cell line derived from epidermoid carcinoma of the larynx, provided by B. van den Hoogen (Erasmus medical center, Rotterdam). HEp-2 cells are widely used for research on virus and respiratory virus. WI-38 cells are fibroblasts derived from human lung tissue, obtained from Sigma (Sigma, #90020107) (57). These cells are often used in virucide testing.

The HEp-2 cells were cultivated in Dulbecco's Modified Eagle's Medium (DMEM) (Sigma, #D6429) enriched with 10% Fetal Bovine serum (FBS) (Sigma, #F7436), 1% Penicillin Streptomycin (PenStrep) (Gibco, #15070063) and 0.7 mM L-Glutamine (Sigma, #G7513). In parallel, WI-38 cells were similarly maintained except that the medium was not supplemented with L-Glutamine. The addition of FBS facilitated cell growth, while PenStrep was used to minimize the bacterial contamination. L-Glutamine was included in the HEp-2 cell culture medium to provide essential nutrients that support cellular metabolism and growth. Both cell lines were incubated at 37 °C in a humidified atmosphere containing 5% CO_2 and were passaged once or twice a week, depending on growth kinetics and confluency.

2.2 Infection with virus

The HEp-2 cells and WI-38 cells were infected with RSV A2 strain provided by B. van den Hoogen (Erasmus medical center, Rotterdam). Prior to infection, the HEp-2 cells and the WI-38 cells were seeded out in 48-wells plate for RT-qPCR and 24-wells plate for Western blot analysis. The HEp-2 cells were seeded out to 40 000 and 80 000 cells per well, while WI-38 cells were seeded out to 35 000 and 70 000 cells per well, respectively. After approximately 24 h, the culture medium was replaced with Opti-MEM (Gibco, #31985047) supplemented with 2% FBS and 0.7 mM L-Glutamine. Subsequently, cells were infected with RSV at a multiplicity of infection (MOI) of 3. Post infection (p.i.), cells were incubated for 12 to 72 hours at 37 °C in a 5% CO_2 atmosphere. The specific duration of incubation time was determined based on the experimental requirements. In certain experiments, supernatant from RSV-infected cells were also collected and stored at -80 °C for further analysis.

2.3 UV-deactivation of virus

RSV A2 provided by B. van den Hoogen was deactivated by UV radiation. UV-deactivated RSV (UV-RSV) was produced by UV-light irradiation of virus stock under controlled fume hood conditions for 1 h. Cells were infected with UV deactivated virus in the same manner described in section 2.2.

2.4 siRNA-mediated gene knockdown (KD)

siRNA can be chemically synthesized to target knockdown (KD) of any gene of interest in mammalian cells. siRNA-mediated KD is achieved through RNA interference where gene expression is suppressed by employing dsRNA such as small interfering RNAs (siRNAs). These siRNAs specifically target and bind to the corresponding mRNA of the gene of interest. Once bound, this interaction leads to the degradation of the mRNA, effectively reducing or silencing the expression of the gene. (58)

siRNA was used to silence cGAS and STING to investigate the contribution of cGAS and STING in RSV-infected WI-38 cells. Specifically, 24 h prior to infection, cells were reverse transfected with siRNA targeting cGAS (ON- TARGETplus Human MB21D1 siRNA, L-015607-02-0005) and STING (ON-TARGETplus Human TMEM172 siRNA, L-024333-00-0005) provided by Dharmacon. These siRNAs were diluted to a working concentration of 1 nM and applied to cells in 24-well plate for Western blot analysis and 48-well plate for RT-qPCR.

Transfection was conducted by using a mixture of Lipofectamin RNAiMAX (0,5 µL) and Opti-MEM (2 µL) for each sample, which was added to the wells. After 15-20 minutes in room temperature, RNAiMAX-siRNA complexes was formed, and WI-38 cells to were added to the plate (35 000 cells/well for RT-qPCR and 70 000 cells/well for Western blot). Following a 24 h period to establish the transfection, selected wells were then infected with RSV at MOI of 3 and incubated for 48 h.

2.5 Infecting cells with RSV-supernatant

Upon infection, RSV utilizes the cellular machinery to transcribe mRNA necessary for production of viral proteins. While RSV mRNA predominantly remains inside the cells,

fragments of viral RNA can leak into the culture medium when infected cells break down. Detection of RSV mRNA in supernatant could serve as an indirect marker of viral replication and dynamics of cellular infection. Consequently, supernatants from infected wells were collected for further analysis and use in subsequent experiments.

The collected supernatant was then used to re-infect HEp-2 cells, which are known for their susceptibility to viral infection and robust proliferation capabilities. For the re-infection process, 15 000 cells per well were seeded out in a 96-well plate and incubated for 24 h. Subsequently, the cells were washed with warm PBS to prepare for exposure to the supernatant. After adding the supernatant, the cells were incubated for additionally 48 h to facilitate re-infection cycle.

2.6 Inhibitors

In order to study the effect of different proteins related to UPR, specific inhibitors were employed. Cells were treated with PERK inhibitor GSK2656157 (#1337532-29-2, MedChemExpress (MCE)) or PKR inhibitor PKR-IN-C16 (#608512-97-6, MedChemExpress (MCE)) 30 min prior to infection with RSV or incubation with medium. The cells were treated with inhibitor at different concentrations, as indicated in the result section.

2.7 Quantitative PCR (qPCR)

Quantitative polymerase chain reaction (qPCR) is a technique used to amplify, detect, and quantify specific DNA or RNA sequences in a sample. During the PCR, the amplifying and accumulation of PCR product is monitored during each cycle of the reaction, allowing precise quantification. The amount of amplified product is measured using fluorescence markers such as SYBR Green, which emits fluorescence when bound to dsDNA. Reverse transcription qPCR (RT-qPCR) is a type of PCR that is used to detect and quantify RNA. Total RNA or mRNA is initially converted into complementary DNA (cDNA) through a process known as reverse transcription. The cDNA serves as a template for quantitative PCR or real time PCR. cDNA is amplified through 20-40 cycles of denaturation, annealing and elongation. The quantity of DNA amplicons in a sample is determined by the intensity of the fluorescent signal emitted after each PCR cycle. The cycle threshold (Ct) is the specific number of cycles required for the fluorescence to surpass a predetermined background level, indicating the presence of target DNA. The Ct value is

inversely proportional to the initial amount of DNA present in the sample, providing a relative measure of quantified DNA.

2.8 RNA-isolation

The cells were lysed with RLT lysis buffer (Qiagen, #7291g) with β-mercaptoethanol (Signa, #M3148). Total RNA was isolated using RNeasy Mini Kit (Qiagen, #74104) following the manufacturers protocol, with additional DNase digestion step. To determine the concentration and purity of the RNA it was used NanoDrop ND-1000 spectrophotometer (Thermo Fisher).

2.9 cDNA-synthesis and RT-qPCR analysis

It was utilized qScript cDNA synthesis Kit (QuantaBio, #95047-100) to reverse transcribe the RNA to cDNA by the manufacturers protocol. Techne CT-512 thermal cycler was used for the synthesis with settings 22 °C for 5 min, 40 °C for 30 min and 85 °C for 5 min. cDNA was diluted 2.5 μg/μL prior to qPCR analysis.

The RT-qPCR analysis was performed at StepOnePlus Real Time PCR System (Applied Biosystems) with the following program settings, 95 °C (20 sec), 95 °C (3 sec) for 40 cycles and 60 °C (30 sec). PerfeCTa SYBR Green Fast mix (QuantaBio, 733-1386) was used for gene analysis. Primer sequences utilized for specific genes are listed in table 2 in the section S.2. Gene expression was quantified by using the ΔΔCt method, by normalizing the sample expression against expression of the endogenous control gene GAPDH for same sample. Fold change was calculated relative to the corresponding non-infected (n.i.) control. RT-qPCR was performed in technical triplicates.

2.11 Western Blot

Western blotting allows for the identification and detection of specific proteins from a complex mixture of proteins extracted from the cells. Proteins are separated based on their molecular weight using SDS-PAGE gel electrophoresis. After separation, the proteins are transferred to a membrane via electrophoresis. Subsequently, the membrane is incubated with antibodies specific to the protein of interest, prior to a secondary antibody conjugated with fluorescent tags that

produces a detectable signal. This allows for visualization of protein bands and quantification of protein by methods such as fluorescence imaging. In this study, Western blot was employed to analyze the protein expression levels of the proteins listed in table 3 and 4 in section S.2.

The cell lysis buffer used for lysing of cells was a 1% lysis buffer solution composed of 50 mM Tris (pH 7.5), 150 mM NaCl, 10% glycerol, 1% Triton X-100 and 2 mM EDTA. The solution was further supplied with phosphatase inhibitor cocktail 2 and 3 (Sigma, #P5726 and #P0044, respectively) and Complete, Mini EDTA-free Protease Inhibitor Cocktail (Sigma, #1183617000). For protein analysis, the extracted proteins were mixed in a 1:3 ratio with NuPAGE 4xLDS Sample buffer (Invitrogen) and DTT reducing agent (0.05 M).

Protein separation was conducted via SDS-PAGE using NuPAGE 4-12 % Bis-Tris gel (1.0 mm x 10 well, Invitrogen) in NuPAGE MOPS SDS running buffer (1X, Invitrogen, #NP0001) at 200 V for approximately 1 h. Protein standards used were See Blue Plus 2 Prestained standard (Invitrogen, #LC5925) and MagicMark XP Western Standard (Invitrogen, #LC5602).

Following electrophoresis, proteins were transferred to a nitrocellulose membrane using Trans-Blot Turbo Transfer Pack with nitrocellulose (Bio-Rad) and Trans-Blot Turbo Transfer System (Bio-Rad), set to high molecular weight settings for 10 min. The membrane was blocked using Intercept Blocking Buffer (Li-Cor, #92760001) and probed with appropriate primary and secondary antibodies. Visualization of protein bands were achieved using LI-COR Odyssey Imager and Image Studio Software (LI-COR Biosciences).

2.12 SA-β-Gal assay

SA-β-gal assay is useful for testing whether different conditions or compounds can induce or inhibit appearance of senescent cells in samples. This is tested through identification of senescence-associated β-galactosidase (SA-β-gal) activity in cells. This enzyme becomes distinctive more active at pH 6.0 in senescent cells, unlike non-senescent cells. For the assay, cells are fixed and strained with a substrate for β-galactosidase such as X-gal, which turns blue when cleaved by the enzyme. The characteristic blue staining provides a visual marker for identifying senescent cells under a microscope. The intensity and distribution of blue color was evaluated for quantification of senescent cells.

The senescence β-galactosidase staining kit (Cell Signaling Technology, #9860) includes essential reagents such as fixation and staining solution along with X-gal. Before using, the reagents are prepared and diluted. Fixation solution is diluted to 1X with distilled water, staining solution is redissolved in 37 °C with agitation prior to being diluted 1X with distilled water. X-gal was dissolved to 20 mg/mL in DMF.

WI-38 cells were seeded out in 12-well plates (140 000 cells/mL). After approximately 24 h, the cells were infected with RSV and incubated for 72 h. The plate was rinsed with 1 mL PBS (5 min) prior to fixation with 1X fixation solution (#11674) for 10-15 min at room temperature. The plate was rinsed with 1 mL PBS (5 x 2 min).

Prior to staining, a mixture of 1 X staining solution, solution A and B and the X-gal stock was made. Each well is added 1 mL X-gal staining solution, consisting of 930 µL 1X staining solution (#11675), 10 µL 100X solution A (#11676), 10 µL 100X solution B (#11677) and 50 µL 20 mg/mL X-gal stock solution (#11678). It is important to check pH levels before staining. The pH levels needs to be 6.0 ±0.1 because high pH levels can cause false negative results. The plate was sealed with parafilm to prevent evaporation and incubated at 37 °C for 24 h in a dry incubator without CO_2 to avoid change in the pH levels. After approximately 24 h, the cells were checked under a microscope (200 X total magnification) to look for development of blue color. Quantification of blue color was done by counting the blue cells in a cross section and dividing that on the number of cells in total in the same section.

2.13 Statistical analysis

Statistical analyses were conducted using GraphPad Prism v10.2.1. The results in figures are presented as mean ± standard error of the mean (SEM). To compare variables between two groups, a Student's T-test was utilized. For comparisons of variables between multiple groups, a One-way ANOVA with Bonferroni's multiple comparison test was applied. Statistical significance was established at a p value of <0.05.

3 Results

Studies in HEp-2 cells

3.1 RSV replication kinetics in HEp-2 cells

HEp-2 cells are derived from human epithelial cells and have been frequently used for RSV replication experiments (59). Initially we characterized RSV kinetics, infecting HEp-2 cells with RSV 12 h, 24 h, 36 h, 48 h, 60 h, and 72 h at multiplicity of infection (MOI) of 3. Detection of RSV fusion protein F_1 and F_1-precursor (F_0) were used to characterize RSV kinetics in HEp-2 cells. The trend observed for RSV F protein was an increase in expression over time (Figure 5). The result demonstrates RSV kinetics in HEp-2 cells.

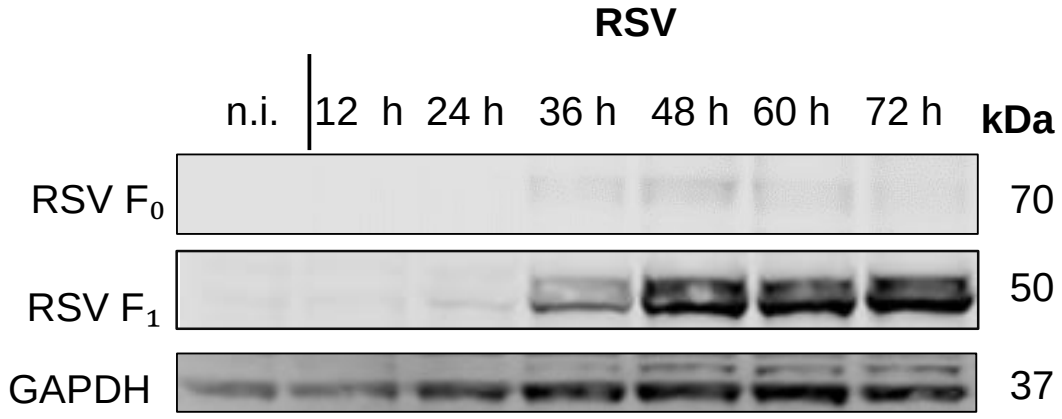

Figure 5: RSV replication kinetics in HEp-2 cells. HEp-2 cells were infected with RSV with a multiplicity of infection (MOI) of 3 for indicated time points (12 h, 24 h, 36 h, 48 h, 60 h or 72 h) or incubated with medium for 24 h (n.i.). Expression of RSV fusion proteins (F_0 and F_1) were examined by Western blotting with GAPDH as endogenous control. Expected molecular weight (kDa) for different proteins are indicated.

3.2 RSV does not induce phosphorylation of eIF2α, but increases expression of CHOP mRNA in HEp-2 cells

Phosphorylation of the eIF2α-subunit contributes to the host cell's defense mechanism against viral infection by inhibiting the protein translation (60). We wanted to establish if RSV infection caused phosphorylation of eIF2α and stimulation of CHOP mRNA in HEp-2 cells, as an indicator of UPR-activation. HEp-2 cells were infected with RSV (MOI 3) for time points ranging from 12 h to 72 h. Evaluation of levels of phosphorylated eIF2α was done by Western blot analysis.

Assessment of CHOP mRNA levels by RT-qPCR was used to indicate if RSV-infected HEp-2 cells stimulates transcription of CHOP mRNA at 48 h post infection. CHOP is a marker for ER-stress and indicator of cellular response to viral infection. The findings indicates that RSV infection does not promote phosphorylation of eIF2α but increases CHOP mRNA expression (Figure 6).

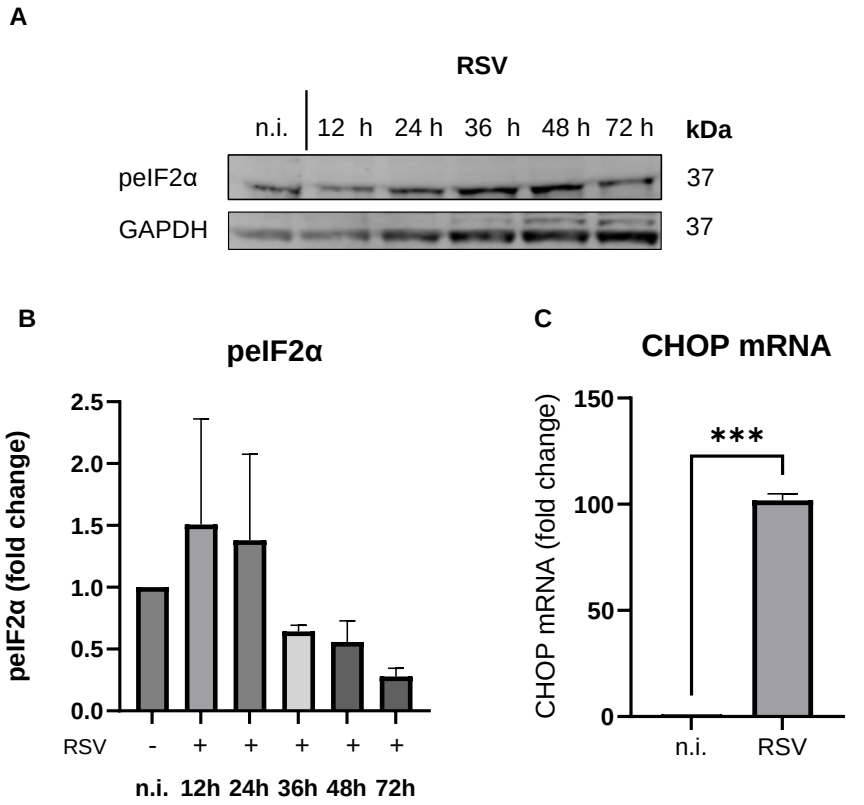

Figure 6: RSV infection induce phosphorylation of eIF2α and expression of CHOP mRNA in HEp-2 cells. (A) HEp-2 cells were infected with RSV with a multiplicity of infection (MOI) of 3 for indicated time points (12 h, 24 h, 36 h, 48 h or 72 h) or incubated with medium for 24 h (n.i.). Expression of peIF2α were assessed by Western blotting with GAPDH as endogenous control. Expected protein weights (kDa) for different proteins are indicated. Protein levels of (B) eIF2α, were quantified, normalized against GAPDH, and presented as fold change relative to the non-infected control. (C) HEp-2 cells were infected with RSV (MOI 3) for 48 h or incubated with medium for 48 h (n.i.). Expression of CHOP mRNA was normalized against GAPDH (endogenous control) and is presented as fold change relative to non-infected cells (n.i.). Data is presented as mean ± SEM for two biological replicates (n=2). Statistical analysis: Two-tailed Student's t-test: *p<0.05, **p<0.01, ***p<0.001, ns: not significant.

3.3 RSV does not stimulate UPR in HEp-2 cells

To evaluate if PERK or PKR was activated by RSV, we examined phosphorylation of PERK and PKR. PERK is primarily activated by ER stress, and PKR is initially activated in response to viral infection and have antiviral effects. To assess if activation of PERK or PKR phosphorylates eIF2α, HEp-2 cells were infected with RSV for 12 h to 72 h with MOI 3. The Western blot analysis indicate minimal change in expression of phosphorylated PERK or PKR for the different times post infection (Figure 7).

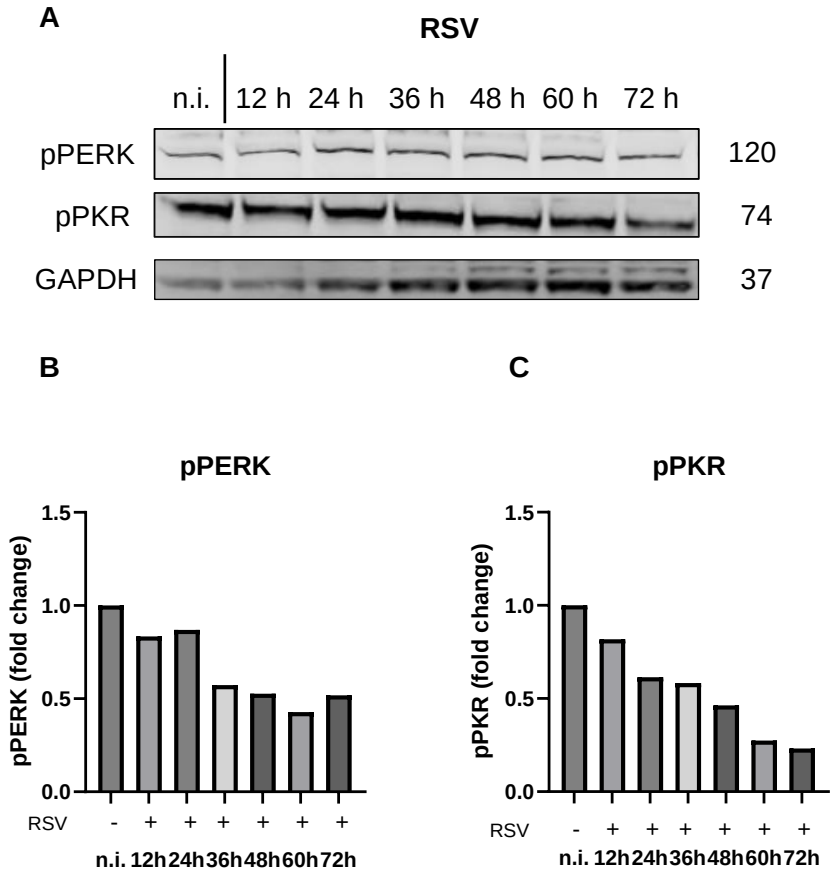

Figure 7: RSV infection does not induce phosphorylation of PERK and PKR in HEp-2 cells. HEp-2 cells were infected with RSV with a multiplicity of infection (MOI) of 3 for indicated time points (12 h, 24 h, 36 h, 48 h or 72 h) or incubated with medium for 24 h (n.i.). Expression of pPERK and pPKR were assessed by Western blotting with GAPDH as endogenous control. Expected protein weights (kDa) for different proteins are indicated. Protein levels of (B) pPERK and (C) pPKR, were quantified, normalized against GAPDH and presented as fold change relative to the non-infected control.

3.4 The effect of PERK inhibitor GSK2656157 on UPR in HEp-2 cells

Zhang et al. conducted experiments in human cells and demonstrated that PERK inhibitor GSK2656157 eliminated STING-initiated eIF2α phosphorylation and disrupted PERK-eIF2α signaling (30). Inspired by these findings, our initial focus was to explore the impact of the PERK inhibitor GSK2656157 in HEp-2 cells infected with RSV. We sought to explore whether the PERK inhibitor affected the UPR through expression of CHOP mRNA and phosphorylation of PERK and eIF2α. The results indicates that the PERK inhibitor did decease expression CHOP mRNA at a concentration of [0.25 μM], however the same reduction was not seen at concentration of [1 μM] (Figure 8 A). The inhibitor had minimal effect on the phosphorylation of eIF2α and PERK (Figure 8 B-D).

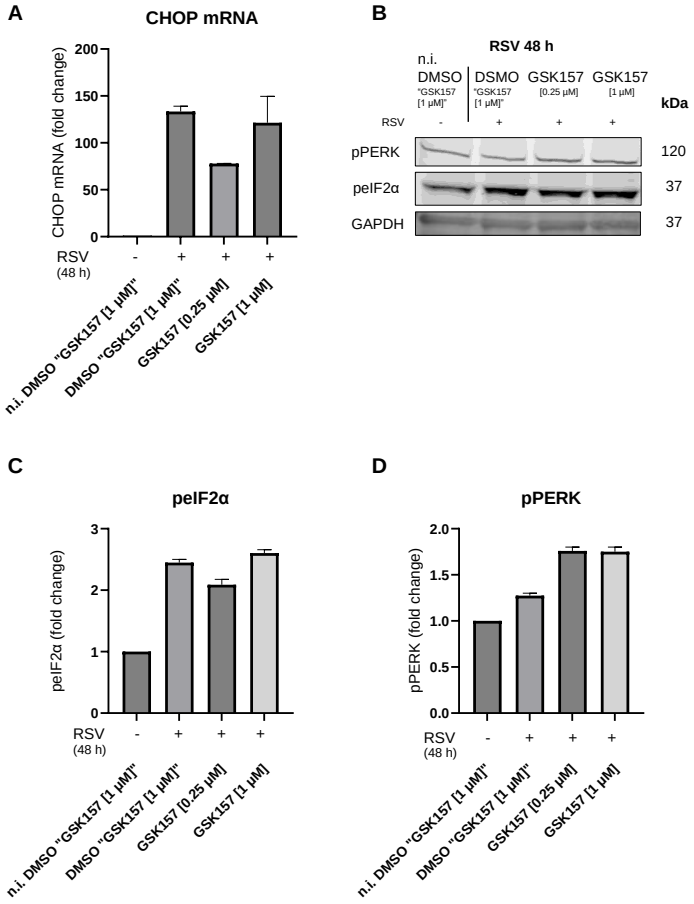

Figure 8: The effect of PERK inhibitor GSK2656157 on UPR in HEp-2 cells. HEp-2 cells were treated with PERK inhibitor GSK2656157 (GSK157) ([0.25 μM or 1 μM]) for 30 min prior to infection with RSV with multiplicity of infection (MOI) of 3 or incubated with medium (n.i.) for 48 h. DMSO controls for the concentration of inhibitor are indicated (DMSO "GSK157 [1 μM]") (A) Expression of CHOP mRNA was normalized against GAPDH (endogenous control) and is presented as fold change relative to non-infected DMSO "GSK157 [1μM". Data is presented as mean ± SEM for two biological replicates (n=2). (B) Expression of peIF2α and pPERK were assessed by Western blotting with GAPDH as endogenous control. Expected protein weights (kDa) for

different proteins are indicated. One representative Western blot for two biological replicates (n = 2) is shown. Protein levels of (C) peIF2α and (D) pPERK, were quantified, normalized against GAPDH and presented as fold change relative to the non-infected control.

The results obtained did not align with initial expectations based on Zhang et al.'s findings, where they observed a significant decrease of eIF2α and eliminated phosphorylation of PERK after treatment with inhibitor (30). Further, we wanted to assess the effect of GSK2656157 on IFN-β and whether the inhibitor fundamentally alters the immune response and specifically target signaling pathways relevant during an RSV infection. RT-qPCR analysis determine decrease in IFN-β mRNA levels after preincubation with PERK inhibitor ([0.25 μM] and [1 μM]) (Figure 9 A). Consequently, it was crucial to investigate if IFN-β levels were decreased due to the PERK inhibitor influencing IFN-β and interferon production in the cell, or if it was due to lower levels of RSV in the cells treated with inhibitor. To assess this, RT-qPCR on RSV N-gene mRNA were performed on the same samples. The analysis revealed that the inhibitor reduced RSV N-gene mRNA levels as well as IFN-β mRNA (Figure 9 B). In addition, RSV F_0 and F_1 protein expression is decreased in samples preincubated with inhibitor (Figure 9 C). In summary, GSK2656157 inhibits production of RSV N-gene mRNA and RSV F_0 and F_1 protein in RSV-stimulated HEp-2 cells. Reduced levels of RSV N-gene mRNA also suggests that reduced level of IFN-β mRNA is due to less viral activity in the cells.

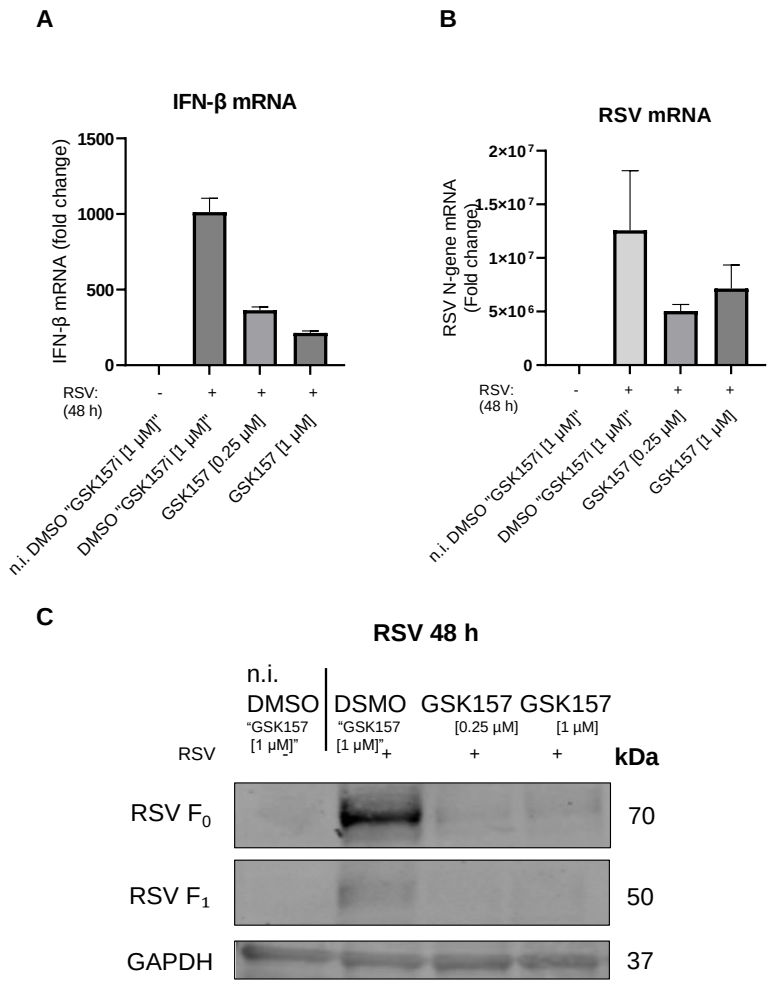

Figure 9: The effect of PERK inhibitor GSK2656157 on IFN-β and RSV N-gene and fusion protein. HEp-2 cells were treated with PERK inhibitor GSK2625157 (GSK157) ([0.25 μM or 1 μM]) for 30 min prior to infection with RSV with multiplicity of infection (MOI) of 3 or incubated with medium (n.i.) for 48 h. DMSO controls for the concentration of inhibitor are indicated (DMSO "GSK157 [1 μM]"). Expression of (A) IFN-β and (B) RSV N-gene mRNA was normalized against GAPDH (endogenous control) and is presented as fold change relative to non-infected DMSO "GSK157 [1μM]". Data is presented as mean ± SEM for two biological replicates (n=2). (C) Expression of RSV fusion proteins (F_0 and F_1) were examined by Western blotting with GAPDH as endogenous control. Expected molecular weight (kDa) for different proteins are indicated. One representative Western blot for two biological replicates (n = 2) is shown.

Studies in WI-38 cells

3.5 RSV is able to replicate in WI-38 cells

RSV primarily targets and infects the epithelial cells lining the airways as well as immune cells (61). Therefore, we wanted to do the same experiments on a more relevant cell type than Hep-2 cells, like lung fibroblasts cells. Initially, we wanted to address if RSV was able to replicate in fibroblasts. To address this, the lung fibroblast cell line WI-38 were infected with RSV for 24 h, 36 h, 48 h, 60 h, and 72 h at MOI 3. The Western blot show that RSV N-gene expression increased with time after infection, and the peak for RSV N-gene was at 72 h p.i (Figure 10).

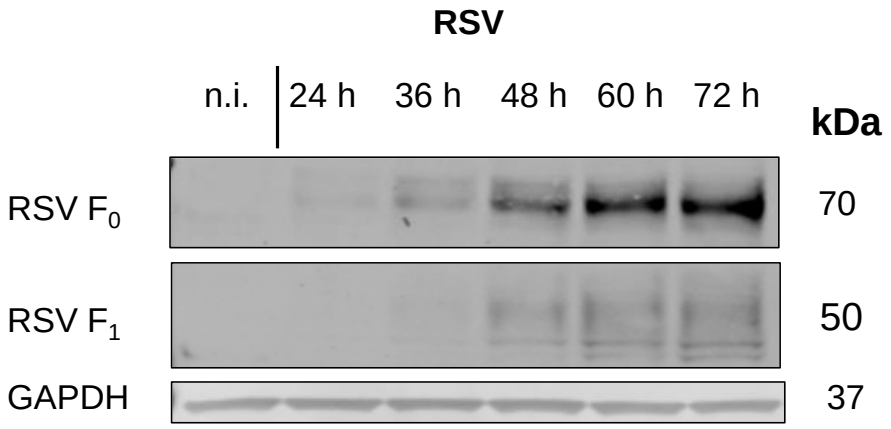

Figure 10:RSV can replicate in WI-38 cells. WI-38 cells were infected with RSV with a multiplicity of infection (MOI) of 3 for indicated time points (24 h, 36 h, 48 h, 60 h or 72 h) or incubated with medium for 24 h (n.i.). Expression of RSV fusion proteins (F_0 and F_1) were examined by Western blotting with GAPDH as endogenous control. Expected molecular weight (kDa) for different proteins are indicated. One representative Western blot for two biological replicates (n = 2) is shown.

3.6 RSV infection stimulate phosphorylation of eIF2α and induction of CHOP mRNA in WI-38 cells

Based on previous results we had already established that RSV infection does not induces phosphorylation of eIF2α and in HEp-2 cells, however, we wanted to investigate if RSV infection revealed the same expression in WI-38 cells. WI-38 cells were infected with RSV at MOI 3 at timepoints ranging from 24 h to 72 h p.i. Western blot analysis indicates a minimal increase in peIF2α after RSV infection (Figure 11 A-B). RT-qPCR analysis revealed a time-dependent increase in CHOP mRNA levels, with the highest peak at 72 h p.i. (Figure 11 C).

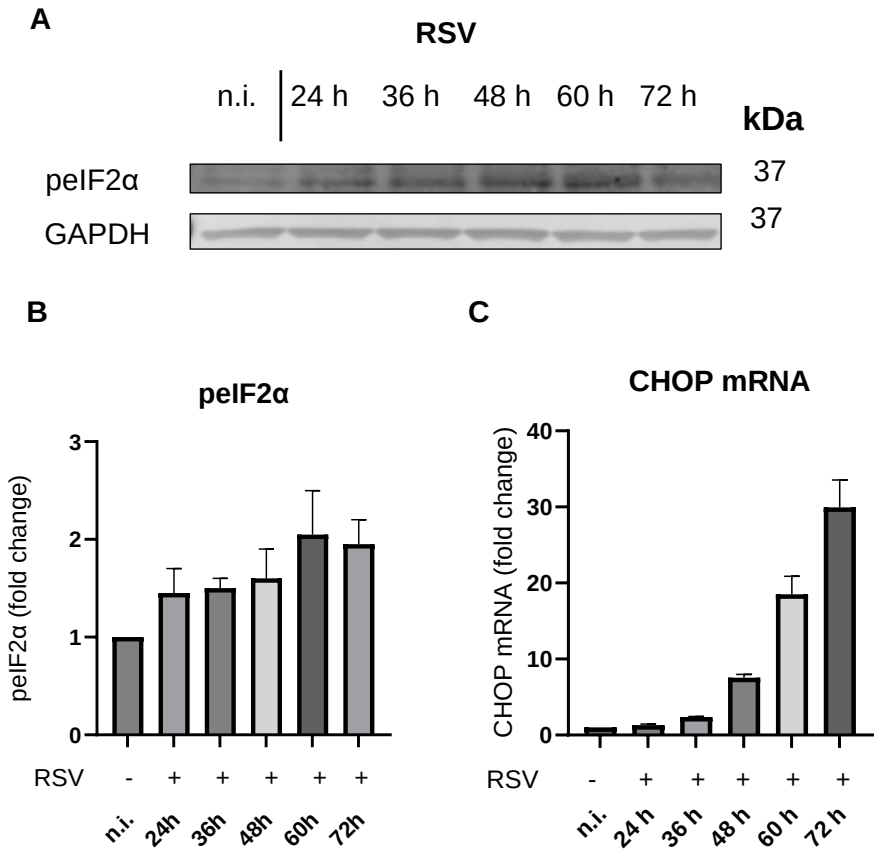

Figure 11: RSV infection induce phosphorylation of eIF2α and expression of CHOP mRNA in WI-38 cells. WI-38 cells were infected with RSV with a multiplicity of infection (MOI) of 3 for indicated time points (24 h, 36 h, 48 h or 72 h) or incubated with medium for 24 h (n.i.). (A-B) Expression of peIF2α were assessed by Western blotting with GAPDH as endogenous control. Expected protein weights (kDa) for different proteins are indicated. One representative Western blot for two biological replicates (n = 2) is shown. Protein levels of (B) peIF2α was quantified, normalized against GAPDH and presented as fold change relative to the non-infected control. (C) Expression of CHOP mRNA was normalized against GAPDH (endogenous control) and is presented as fold change relative to non-infected cells (n.i.). Data is presented as mean ± SEM for two biological replicates (n=2).

3.7 RSV affects UPR in WI-38 cells

Equally to HEp-2 cells, we wanted to investigate phosphorylation of PERK or PKR in WI-38 cells. WI-38 cells were infected with RSV (MOI 3) for 24 h to 72 h and Western blot was used to assess phosphorylation of PKR and PERK. Western blot analysis indicated that RSV did not phosphorylate PERK (Figure A-B). We found that PKR is phosphorylated in WI-38 cells infected with RSV, and the phosphorylation increases correlating to time p.i., with a peak at 48 to 60 h p.i. (Figure 12 C). Furthermore, we aimed to extend our investigation to examine the unfolded protein response (UPR) in WI-38 cells (Figure 4).

The main purpose of UPR is to restore normal function of ER in the cell. We wanted to investigate if UPR was activated by RSV infection. This was done by RT-qPCR on UPR genes XBP1 spliced and unspliced (respectively XBP1s and XBP1us), IRE1 and ATF6 (Figure 12 D-G). The results demonstrate that all UPR genes except XBP1us have a peak in mRNA expression at 72 h p.i, and XBP1us have a peak at 60 h p.i. The increase in ATF6 mRNA was minimal. These increases correlate with increase in expression of RSV N-gene (Figure 10) and induction of CHOP (Figure 11), which also is a UPR gene. This suggests that RSV activates components of UPR after infection.

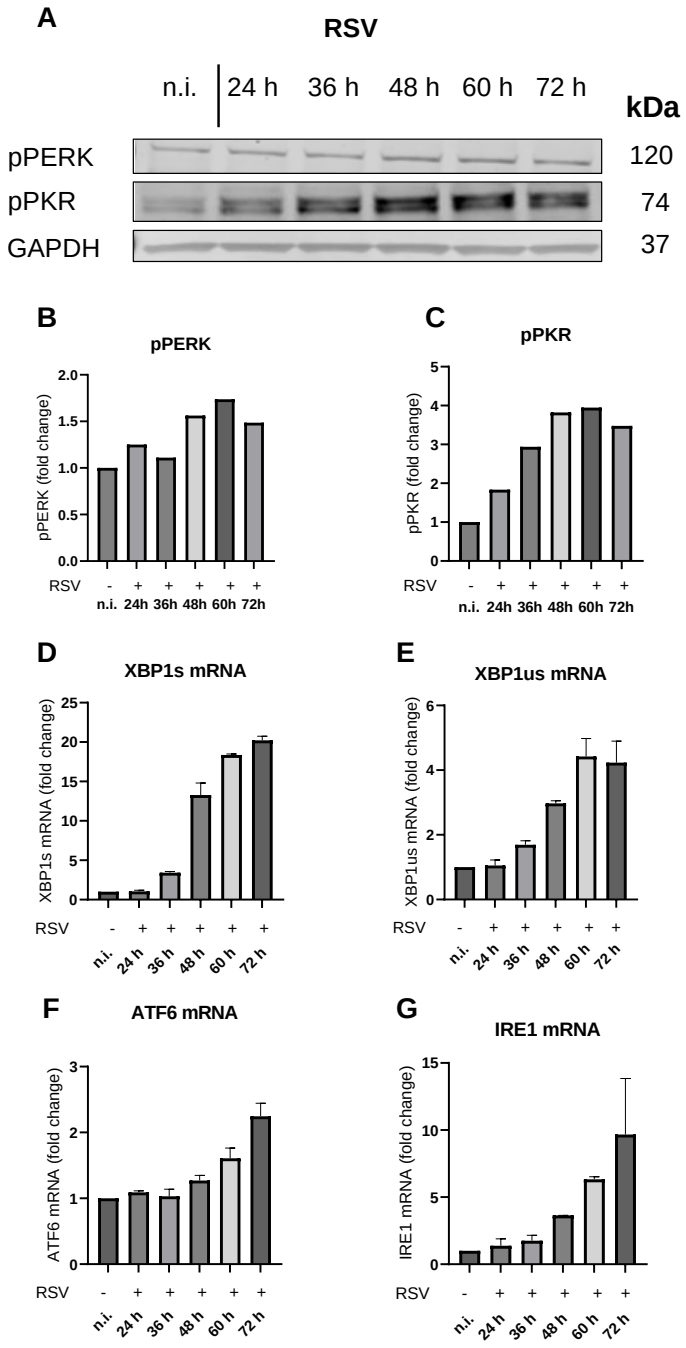

Figure 12: RSV affects UPR in WI-38 cells. WI-38 cells were infected with RSV with a multiplicity of infection (MOI) of 3 for indicated time points (24 h, 36 h, 48 h or 72 h) or incubated with medium for 24 h (n.i.). (A-C) Expression of pPERK and pPKR were assessed by Western blotting with GAPDH as endogenous control. Expected protein weights (kDa) for different proteins are indicated. One representative Western blot for two biological replicates (n = 2) is shown. Protein levels of (B) pPERK and (C) pPKR was quantified, normalized against GAPDH and presented as fold change relative to the non-infected control. (D) Expression of XBP1s mRNA was normalized against GAPDH (endogenous control) and is presented as fold change relative to non-infected cells (n.i.). (E) Expression of XBP1us mRNA was normalized against GAPDH (endogenous control) and is presented as fold change relative to non-infected cells (n.i.). (F) Expression of ATF6 mRNA was normalized against GAPDH (endogenous control) and is presented as fold change relative to non-infected cells (n.i.). (G) Expression of IRE1 mRNA was normalized against GAPDH (endogenous control) and is presented as fold change relative to non-infected cells (n.i.). Data is presented as mean ± SEM for two biological replicates (n=2).

3.8 Phosphorylation of eIF2α and PKR depends on RSV replication in WI-38 cells

Earlier results suggested that RSV does not phosphorylate PERK, however we wanted to investigate whether phosphorylation of PKR is dependent on RSV replication. This was done by infecting WI-38 cells with RSV and UV-deactivated RSV (UV-RSV) for 48 and 72 h (Figure 13). Inactivation of virus with UV-radiation blocks the virus's ability to replicate. The dramatically decrease in RSV fusion protein expression imply successful UV-deactivation. eIF2α is phosphorylated in replicating RSV, but not in samples infected with UV-deactivated RSV. Suggesting that phosphorylation of eIF2α is dependent on replicating RSV. In addition, phosphorylation of PKR was less expressed for samples infected with UV-deactivated RSV in WI-38 cells. This suggests that phosphorylation of eIF2α is more dependent on activation of PKR than PERK.

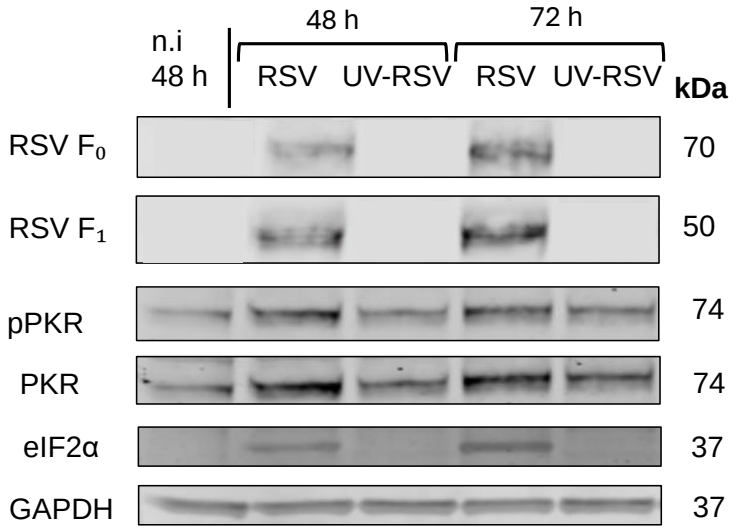

Figure 13: Phosphorylation of eIF2α and PKR depends on RSV replication in WI-38 cells. WI-38 cells were infected with RSV with a multiplicity of infection (MOI) or UV deactivated RSV for 48 to 72 h or incubated with medium for 48 h (n.i.). Expression of pPERK, pPKR, PKR, RSV fusion protein (F_0 and F_1), peIF2α were assessed by Western blotting with GAPDH as endogenous control. Expected protein weights (kDa) for different proteins are indicated. One representative Western blot for two biological replicates (n = 2) is shown

3.9 The effect of PERK inhibitor GSK2656157 on UPR in RSV-infected WI-38 cells

We had already conducted experiments using the GSK2656157 PERK inhibitor in HEp-2 cells, but we wanted to elucidate the effects of the inhibitor in WI-38 cells as well, since these are more relevant for respiratory infection. The cells were treated with GSK2656157 ([0.25 μM] and [1

μM]) prior to infection with RSV (MOI 3) for 48 h. We sought to explore whether the PERK inhibitor affected phosphorylation of eIF2α and PERK and induction of CHOP. The analysis indicates that peIF2α and pPERK is not affected by the inhibitor, independent on increased concentrations (Figure 14 A-B). The same results were found for CHOP mRNA expression (Figure 14 C-D). This confirmed that we did not observe phosphorylation of PERK after RSV infection in section 3.7 (Figure 12 A-B).

RT-qPCR on IFN-β and RSV N-gene was conducted to investigate how the inhibitor affects the fundamental immune response and viral replication. The RT-qPCR analysis indicated no significant difference in IFN-β mRNA levels after treatment with PERK inhibitor (Figure 15 A) and that the inhibitor does not have a significant effect on RSV N-gene mRNA levels (Figure 15 B). However, RSV F_0 and F_1 protein expression is decreased to some degree in sample with PERK inhibitor [1 μM] (Figure 15 C-D).

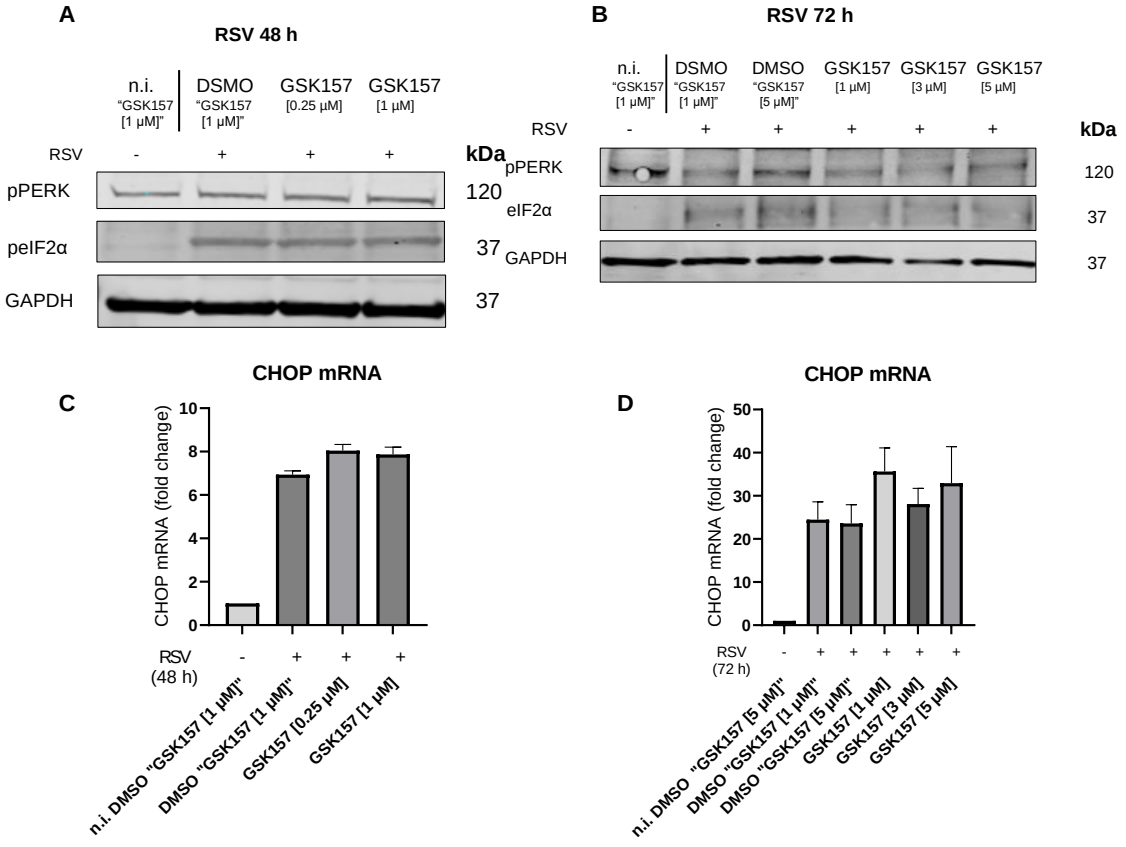

Figure 14: The effect of PERK inhibitor GSK2656157 on UPR in RSV-infected WI-38 cells. WI-38 cells were treated with PERK inhibitor GSK2625157 (GSK157) ([0.25 μM], [1 μM] [3 μM] or [5 μM]) for 30 min prior to infection with RSV with multiplicity of infection (MOI) of 3 and incubated with medium (n.i.) for 48 or 72 h. DMSO controls for two concentration of

inhibitor are indicated (DMSO "GSK157 [1μM]" and DMSO "GSK157 [5μM]") (A) and (B) Expression of peIF2α and pPERK were assessed by Western blotting with GAPDH as endogenous control. Expected protein weights (kDa) for different proteins are indicated. (C-D) Expression of CHOP mRNA was normalized against GAPDH (endogenous control) and is presented as fold change relative to non-infected DMSO "GSK157 [1μM). Data is presented as mean ± SEM for two biological replicates (n=2).

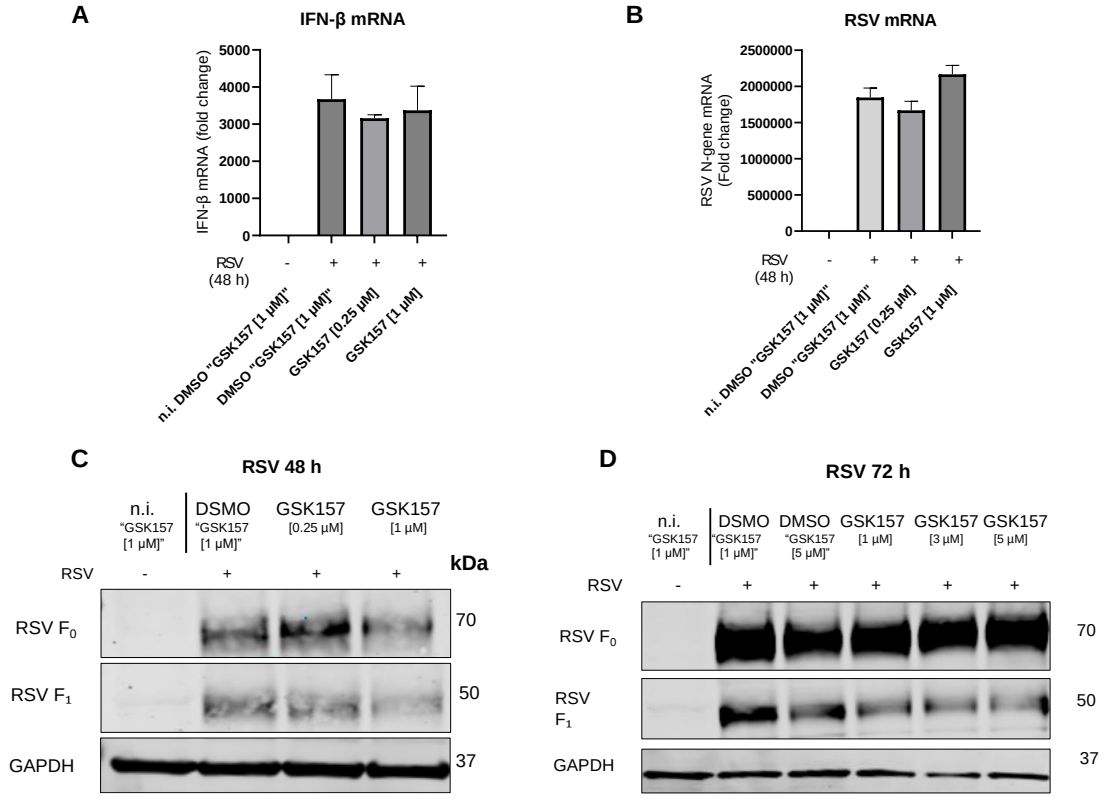

Figure 15: The effect of PERK inhibitor GSK2656157 on UPR in RSV-infected WI-38 cells. WI-38 cells were treated with PERK inhibitor GSK2656157 (GSK157) ([0.25 μM, [1 μM] [3 μM] or [5 μM]) for 30 min prior to infection with RSV with multiplicity of infection (MOI) of 3 or incubated with medium (n.i.) for 48 h or 72 h. DMSO controls for the concentration of inhibitor are indicated (DMSO "GSK157 [1μM]"). Expression of (A) IFN-β and (B) RSV N-gene mRNA was normalized against GAPDH (endogenous control) and is presented as fold change relative to non-infected DMSO "GSK157 [1μM]". Data is presented as mean ± SEM for two biological replicates (n=2). Expected protein weights (kDa) for different proteins are indicated. (C-D) Expression of RSV fusion proteins (F_0 and F_1) were examined by Western blotting with GAPDH as endogenous control. Expected molecular weight (kDa) for different proteins are indicated. One representative Western blot for two biological replicates (n = 2) is shown.

3.10 PKR-inhibitor PKR-IN-C16 reduces RSV-stimulated peIF2α and UPR in WI-38 cells

Considering that our previous results indicated that the PERK inhibitor GSK2656157 did not have significant effect on UPR in RSV-stimulated WI-38 cells. We were interested to investigate if inhibiting PKR with PKR-IN-C16 (C16) affected UPR in WI-38 cells after infection with RSV. The PKR-IN-C16 binds to PKR and inhibits autophosphorylation of PKR. Prior to infection, the cells were treated with PKR-IN-C16 ([1 μM], [3 μM] or [5 μM]) and then infected with RSV (MOI 3) for 72 h. Expression levels of peIF2α, pPKR and PKR protein were decreased in

samples treated with PKR inhibition [3 µM] and [5 µM] (Figure 16 A). RT-qPCR analysis suggest significant decrease in CHOP and XBP1s mRNA in cells treated with inhibitor ([3µM] and [5µM]) compared to respective RSV-infected DMSO control (DMSO "PKR-IN-C16 [5 µM]" (Figure 16 B-C). Collectively, this suggests that the inhibitor affects activation of PKR and eIF2α and induction of CHOP and XBP1s mRNA.

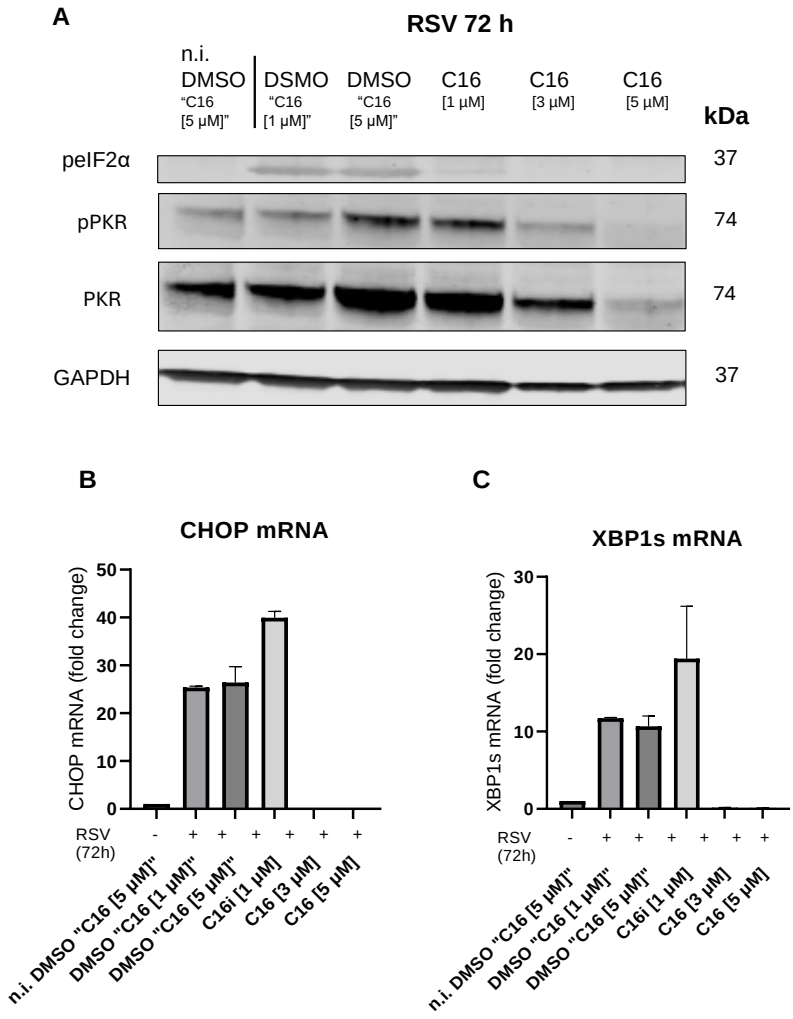

Figure 16: PKR inhibitor PKR-IN-C16 inhibits UPR in WI-38 cells. WI-38 cells were treated with PKR-inhibitor PKR-IN-C16 (C16) ([1 µM], [3µM] or [5 µM]) for 30 min prior to infection with RSV with multiplicity of infection (MOI) of 3 or incubated with medium (n.i.) for 72 h. DMSO controls for two concentrations of inhibitor are indicated (DMSO "C16 [1µM]" and DMSO "C16 [5µM]"). (A) Expression of peIF2α, pPKR and PKR were assessed by Western blotting with GAPDH as endogenous control. Expected protein weights (kDa) for different proteins are indicated. One representative Western blot for two biological replicates (n = 2) is shown. Expression of (B) CHOP mRNA and (C) XPB1swas normalized against GAPDH (endogenous control) and is presented as fold change relative to non-infected DMSO "C16 [5 µM)".Data is presented as mean ± SEM for two biological replicates (n=2).

RT-qPCR analysis indicated reduction in IFN-β mRNA with increased concentrations of the inhibitor (Figure 17 A). Inhibition of PKR caused an increase in fold change for RSV N-gene, especially PKR-IN-C16 [3 µM] (Figure 17 B). In contrast, Western blot analysis indicate that the PKR-IN-C16 [3 µM] inhibits production of RSV F_0 and F_1 protein (Figure 17 C). Notably, reduced cell confluency was observed after treatment with PKR inhibitor.

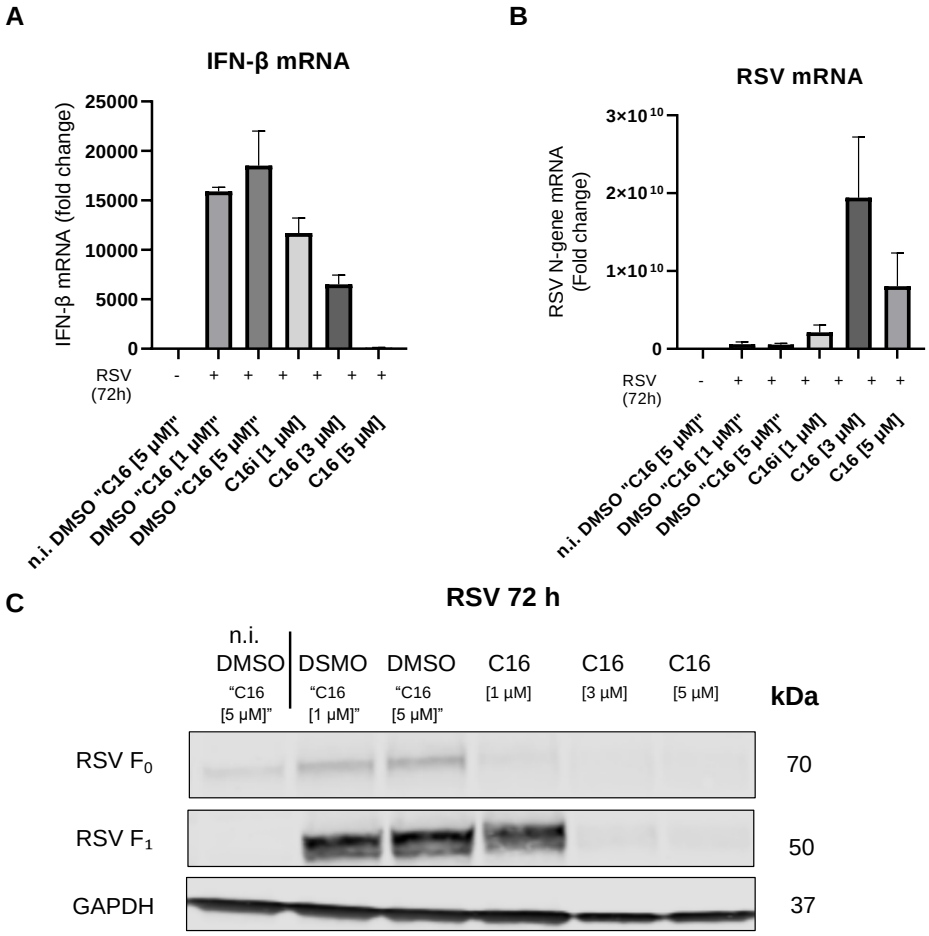

Figure 17: The effect of PKR inhibitor PKR-IN-C16 on RSV and IFN-β mRNA in WI-38 cells. WI-38 cells were treated with PRK-inhibitor PKR-IN-C16 (C16) ([1 µM, 3 µM] or [5 µM]) for 30 min prior to infection with RSV with multiplicity of infection (MOI) of 3 or incubated with medium (n.i.) for 72 h. DMSO controls for the concentration of inhibitor are indicated (DMSO "C16 [1 µM]" or DMSO "C16 [5 µM]"). (A) Expression of IFN-β mRNA and (B) RSV N-gene was normalized against GAPDH (endogenous control) and is presented as fold change relative to non-infected (DMSO "C16 [1µM]"). Data is presented as mean ± SEM for two biological replicates (n=2). (C) Expression of RSV fusion proteins (F_0 and F_1) were examined by Western blotting with GAPDH as endogenous control. Expected molecular weight (kDa) for different proteins are indicated. One representative Western blot for two biological replicates (n = 2) is shown.

3.11 Assessment of viral mRNA in supernatant after RSV infection

We wanted to investigate if it was viral mRNA in the supernatant from samples with infectious RSV and UV-irradiated RSV. Viral mRNA in the supernatant could mean that the virus causes damage to the cell, leading to release of viral mRNA into the supernatant. We established a method for reinfecting cells with supernatant to assess if it was possible to detect infectious RSV in supernatant from WI-38 cells and HEp-2 cells. We infected HEp-2 cells with supernatant because we knew these cells responded well to active RSV infection. RT-qPCR was assessed to detect that RSV in supernatant in WI-38 cells and in HEp-2 cells can replicate and reinfect HEp-2 cells (Figure 18). We also determined that supernatant from UV-deactivated RSV is not infectious.

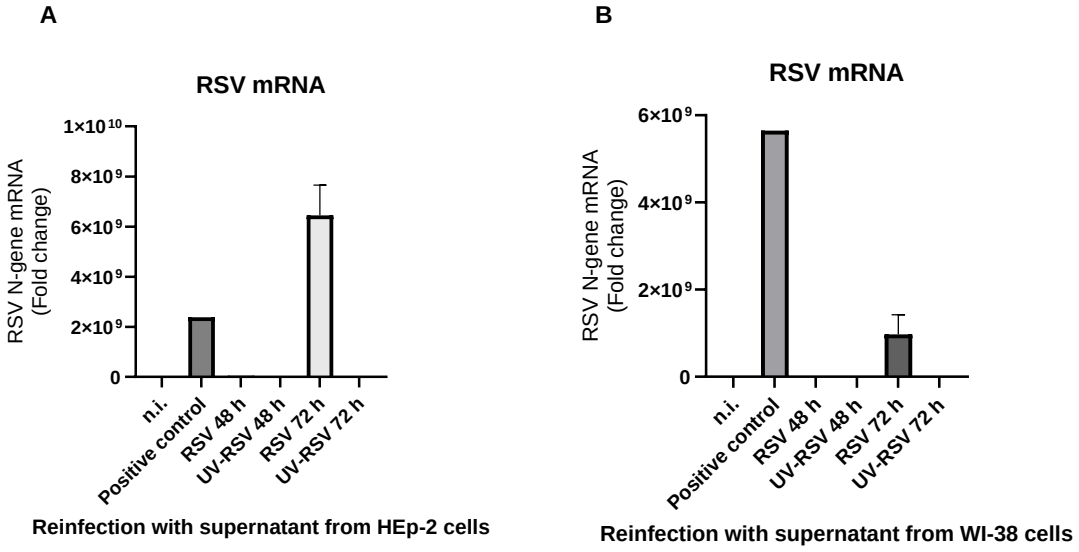

Figure 18: **Assessment of viral mRNA in supernatant after RSV infection.** HEp-2 cells were reinfected with supernatant with infectious RSV or UV-irradiated RSV from either HEp-2 cells or from WI-38 cells. Lysate from HEp-2 cells infected with RSV was used as positive control. (A) Expression of RSV N-gene mRNA in cells reinfected with supernatant from HEp-2 cells was normalized against GAPDH (endogenous control) and is presented as fold change relative to non-infected cells (n.i.). (B) Expression of RSV N-gene mRNA in cells reinfected with supernatant from WI-38 cells was normalized against GAPDH (endogenous control) and is presented as fold change relative to non-infected cells (n.i.) Data is presented as mean ± SEM for two biological replicates (n=2).

3.12 siRNA-mediated KD of cGAS and STING

To examine if signaling through cGAS and STING affects RSV replication and reproduction, we established siRNA-mediated KD of cGAS and STING in WI-38 cells. siRNA concentrations of 10 nM and transfection time of 24 h were assessed. RT-qPCR was assessed to examine

expression of cGAS and STING mRNA in samples undergone siRNA-mediated KD of cGAS or STING in medium and in samples infected with RSV for 48 h. cGAS and STING mRNA were significantly decreased in samples incubated in medium and in samples infected with RSV (Figure 19 A-D). Western blot analysis indicated KD of cGAS and STING protein corresponding to mRNA expression from RT-qPCR (Figure 19 E). KD-efficiency (%) was calculated to > 80% in all samples and was considered successful (Table 1, section S.1)

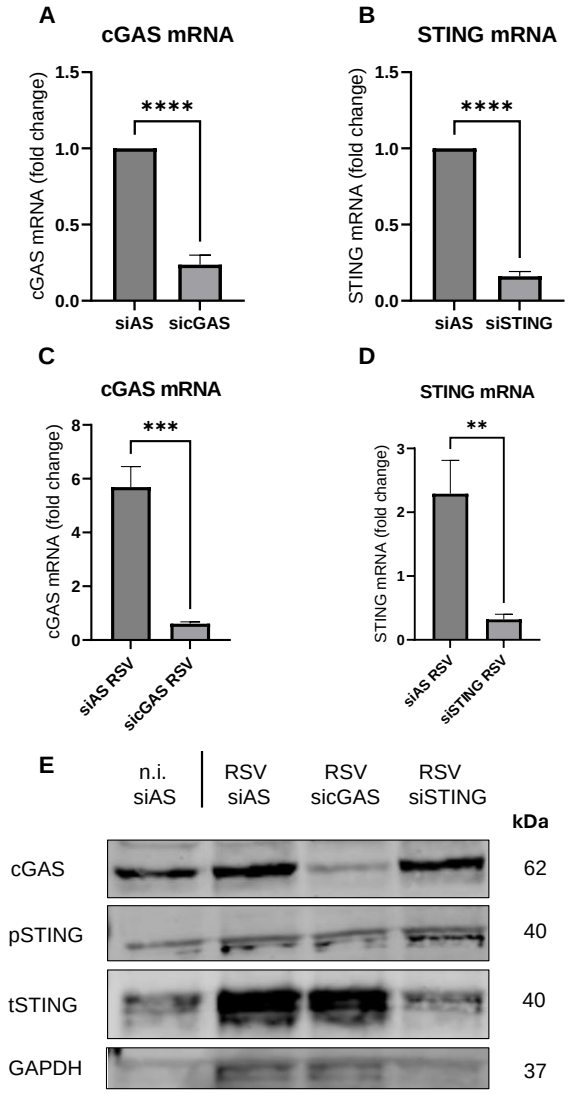

Figure 19: siRNA mediated KD of cGAS and STING. WI-38 cells were reversed transfected with control siRNA siAllStar (siAS), siSTING or sicGAS with a concentration of 10 nM and transfection time of 24 h prior to infection with RSV with a multiplicity of infection (MOI) of 3 for 48 h after. Expression of (A, C) cGAS and (B, D) STING mRNA expression was normalized against GAPDH (endogenous control) and is presented as fold change relative to siAS transfected cells. Data is presented as mean ± SEM for four biological replicates (n=4). (E) Expression of cGAS and STING was analysed by Western Blot with GAPDH as endogenous control. Expected molecular weight (kDa) for different proteins are indicated. Statistical analysis: Two-tailed Student's t-test: *p<0.05, **p<0.01, ***p<0.001, ns: not significant.

3.13 cGAS and STING activation in UPR in Wi-38 cells

Zhang et al. reported that STING induces PERK-mediated eIF2α phosphorylation (30). To evaluate it the cGAS-STING axis impacted on eIF2α and UPR in RSV-infected cells, siRNA-mediated KD of cGAS and STING was performed. siRNA concentrations of 10 nM and transfection time of 24 h and infection with RSV for 48 h were assessed. Western blot analysis revealed that phosphorylation of eIF2α, PERK or PKR were not affected by siRNA-mediated KD of cGAS and STING. RT-qPCR revealed that siRNA-mediated KD of STING had minimal effect on CHOP mRNA, however, sicGAS did increase mRNA levels of CHOP (Figure 20). RSV N-gene mRNA was not significantly decreased (Figure 21). Correspondingly, our results suggests that cGAS- and STING-depleted cells does not significantly affect expression of RSV F_0 or F_1.

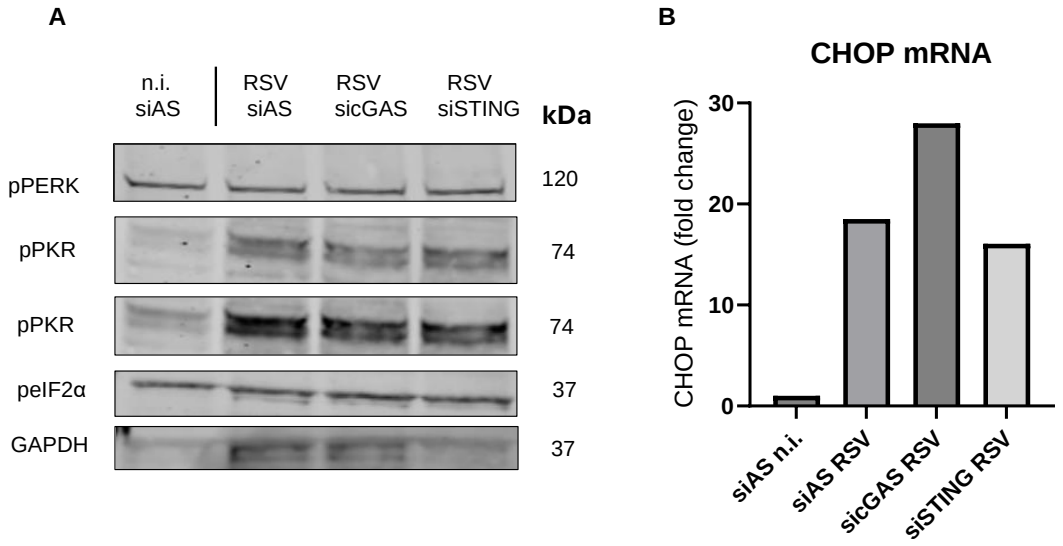

Figure 20: siRNA mediated KD of cGAS and STING does not affect UPR. WI-38 cells were reversed transfected with control siRNA siAllStar (siAS), siSTING or sicGAS with a concentration of 10 nM and transfection time of 24 h. (A) Expression of pPERK, pPKR, PKR and eIF2α was analyzed by Western Blot with GAPDH as endogenous control. Expected molecular weight (kDa) for different proteins are indicated. (B) Expression of CHOP mRNA was normalized against GAPDH (endogenous control) and is presented as fold change relative to non-infected (n.i) siAS transfected cells.

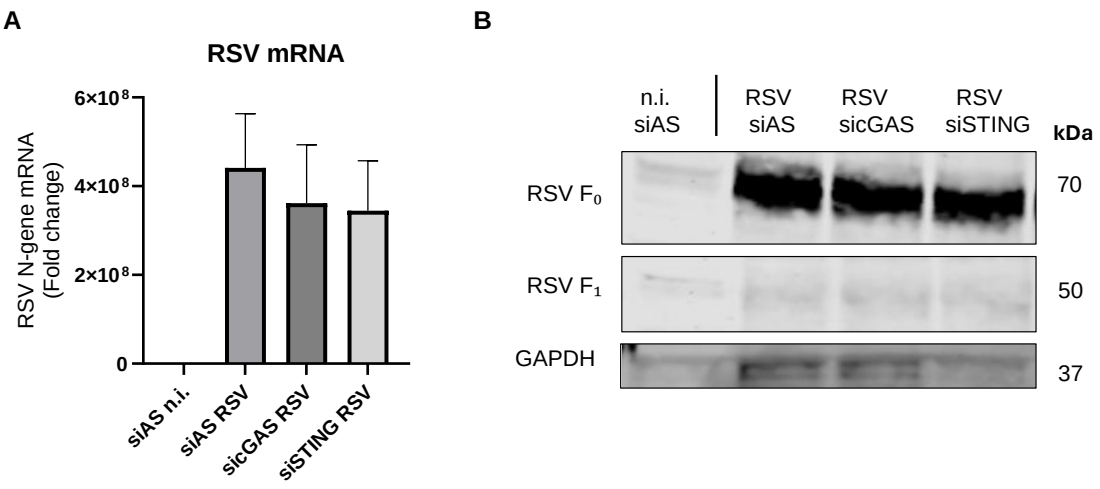

Figure 21: siRNA mediated KD of cGAS and STING does not affect RSV. WI-38 cells were reversed transfected with control siRNA siAllStar (siAS), siSTING or sicGAS with a concentration of 10 nM and transfection time of 24 h prior to infection with RSV with a multiplicity of infection (MOI) of 3 for 48 h after. Expression of (A) RSV N-gene mRNA was normalized against GAPDH (endogenous control) and is presented as fold change relative to siAS transfected cells. Data is presented as mean ± SEM for four biological replicates (n=4). (B) Expression of RSV fusion proteins (F_0 and F_1) were examined by Western blotting with GAPDH as endogenous control. Expected molecular weight (kDa) for different proteins are indicated.

3.14 RSV induces senescence in WI-38 cells

UPR activation has been associated with the induction of senescence (62). As we observed UPR activation in RSV-infected WI-38 cells, we wanted to evaluate if RSV can induce senescence. Senescence was detected by senescence-associated β-galactosidase (SA-β-gal) assay. WI-38 cells were incubated in medium or infected with RSV for 72 h prior to staining. The cells were stained with X-gal chromogen, a direct substrate for β-galactosidase. When X-gal chromogen reacts with β-galactosidase in the senescent cell, the product oxidizes to a blue substance, which is a visual analysis of β-galactosidase activity in the cells (54). The cells were analyzed with a light microscopy with total magnification of 200x (Figure 22 A-B). The senescence was quantified as a percentage of blue colored cells (Figure 22 C). There is a significant increase in senescence in the cells infected with RSV compared to uninfected cells.

H3K9me3 is a histone modification that plays a role in the process and maintenance of cellular senescence and works as a marker for senescence (63). WI-38 cells were infected with RSV for 24 to 72 h. The analysis revealed that expression of H3K9me3 increases correlating to time p.i, with a peak at 72 h p.i (Figure 22 D).

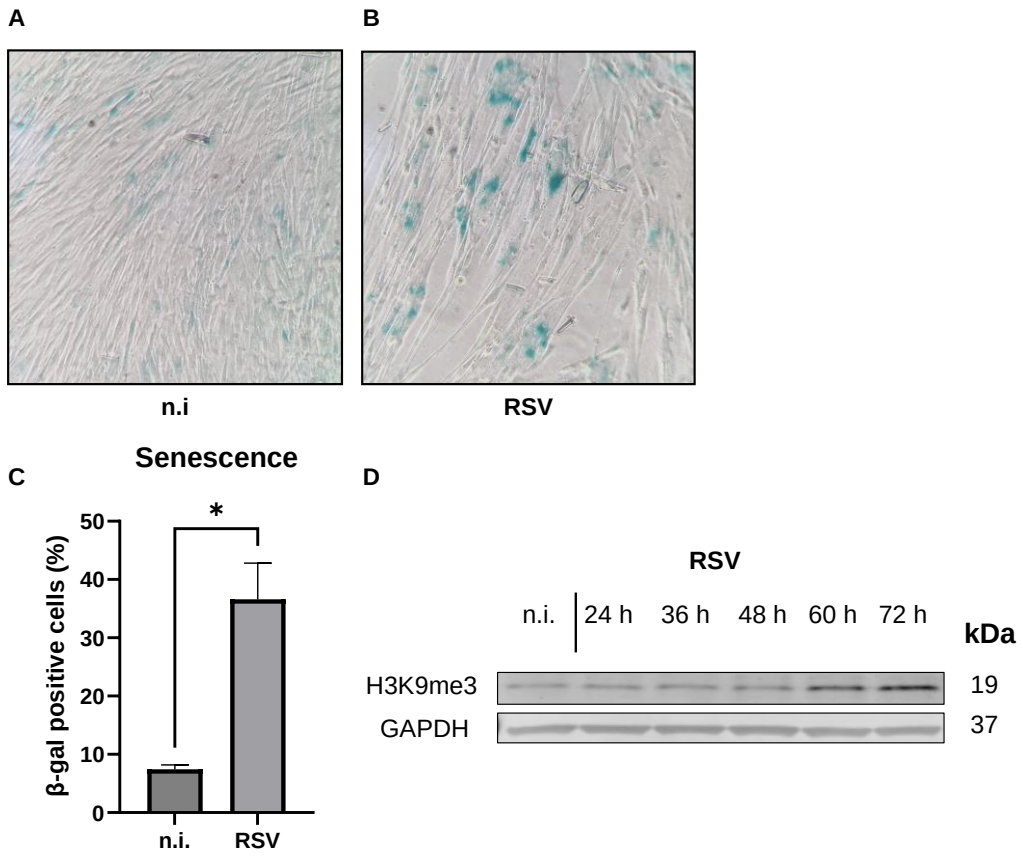

Figure 22: RSV induced senescence in WI-38 cells. WI-38 cells were infected with RSV with a multiplicity of infection (MOI) of 3 for indicated time points (24 h, 36 h, 48 h or 72 h) or incubated with medium for 24 h (n.i.). (A) Light microscopic image of senescent cells stained blue using senescence-associated β-galactosidase (SA- β-gal) assay in non-infected (n.i) cells and (B) cells infected with RSV with a multiplicity of infection (MOI) 3 for 72 h. The photographs were taken at total magnification 200x. (C) WI-38 cells were infected with RSV with a multiplicity of infection (MOI) of 3 or incubated with medium for 72 h (n.i.). Senescence was detected by SA- β-gal and quantified as the amount of blue colored cells as a percentage of cells in total. Data is presented as mean ± SEM for two biological replicates (n=2). Statistical analysis: Two-tailed Student's t-test: *p<0.05, **p<0.01, ***p<0.001, ns: not significant. (D) Expression of H3K9me3 was normalized against GAPDH (endogenous control) and is presented as fold change relative to non-infected (n.i) cells. One representative Western blot for two biological replicates (n = 2) is shown.

3.15 PKR inhibitor PKR-IN-C16 prevents RSV-induced senescence in WI-38 cells

Subsequently, we aimed to examine it RSV induces senescence through UPR. WI-38 cells were treated with PKR inhibitor PKR-IN-C16 ([3 μM]) and PERK inhibitor GSK2656157 ([1 μM]) prior to RSV infection (MOI 3) for 72 h. The analysis indicates that the PERK inhibitor GSK2656157 did not affect senescence in WI-38 cells infected with RSV, but the PKR inhibitor decreased senescence significantly (Figure 23 A). For further investigation, we examined the effect of PKR inhibitor at different concentrations. We treated the cells with PKR-IN-C16

inhibitor ([0.5 µM], [1 µM], [3 µM] or [5 µM]) prior to RSV infection (MOI 3) for 72 h. The analysis indicate that the inhibitor decreases senescence in WI-38 cells infected with RSV significantly, independent of the concentration we used (Figure 23 B). Notably, reduced cell confluency was observed after treatment with PKR inhibitor (Figure 24).

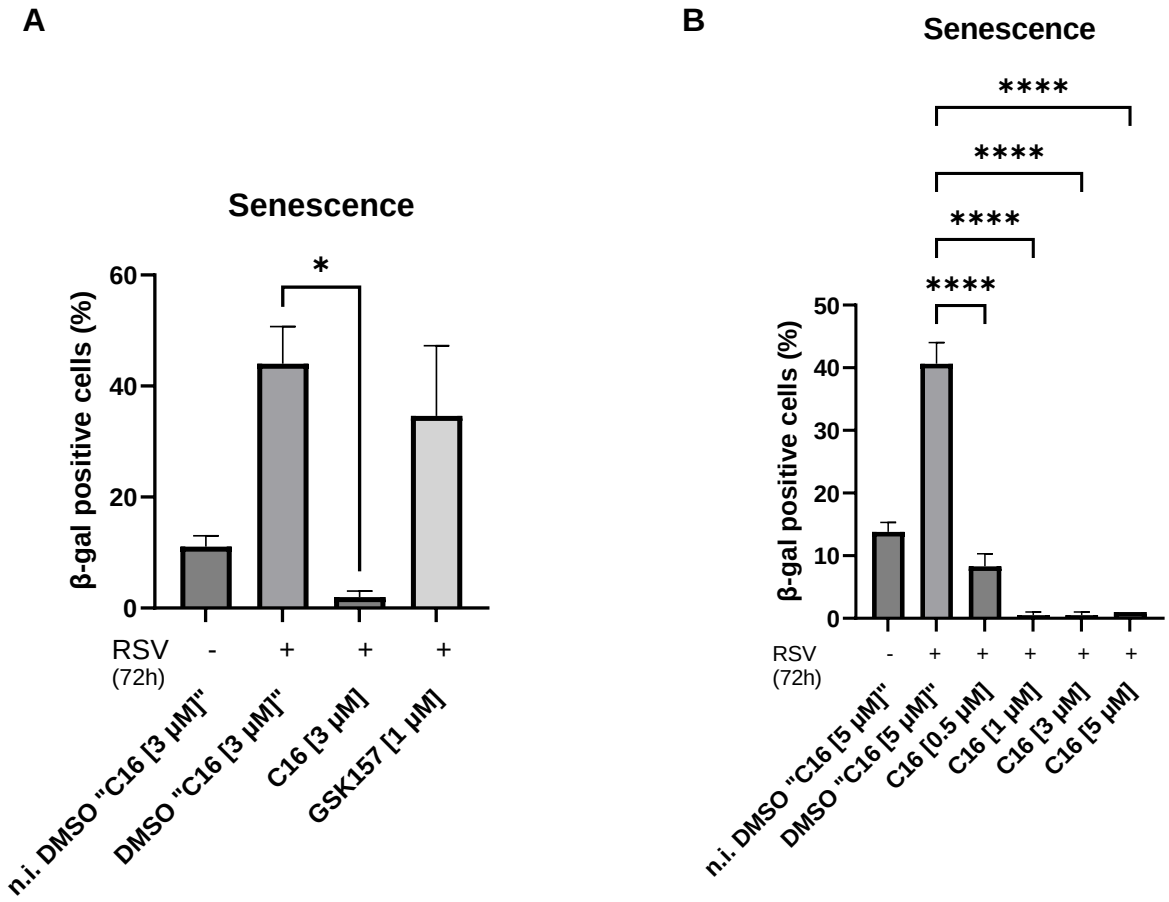

Figure 23: PKR-IN-C16 prevents senescence in WI-38 cells. (A) WI-38 cells were treated with PKR inhibitor PKR-IN-C16 and PERK inhibitor for 30 min prior to infection with RSV with multiplicity of infection (MOI) of 3 or incubated with medium (n.i.) for 72 h. DMSO controls for concentration of inhibitor are indicated (DMSO "C16 [3 µM]"). (B) WI-38 cells were treated with PKR-inhibitor PKR-IN-C16 (C16) ([0.5 µM], [1 µM], [3 µM] or [5 µM]) for 30 min prior to infection with RSV with multiplicity of infection (MOI) of 3 or incubated with medium (n.i.) for 72 h. DMSO controls for concentration of inhibitor are indicated (DMSO "C16 [5 µM]"). Senescence was detected by senescence-associated β-galactosidase (SA-β-gal) assay and quantified as the amount of blue colored cells as a percentage of cells in total. Data is presented as mean ± SEM for two biological replicates (n=2). Statistical analysis: One way ANOVA with Bonferroni's multiple comparisons test: *p<0.05, **p<0.01, ***p<0.001, ****p<0.0001, ns: not significant.

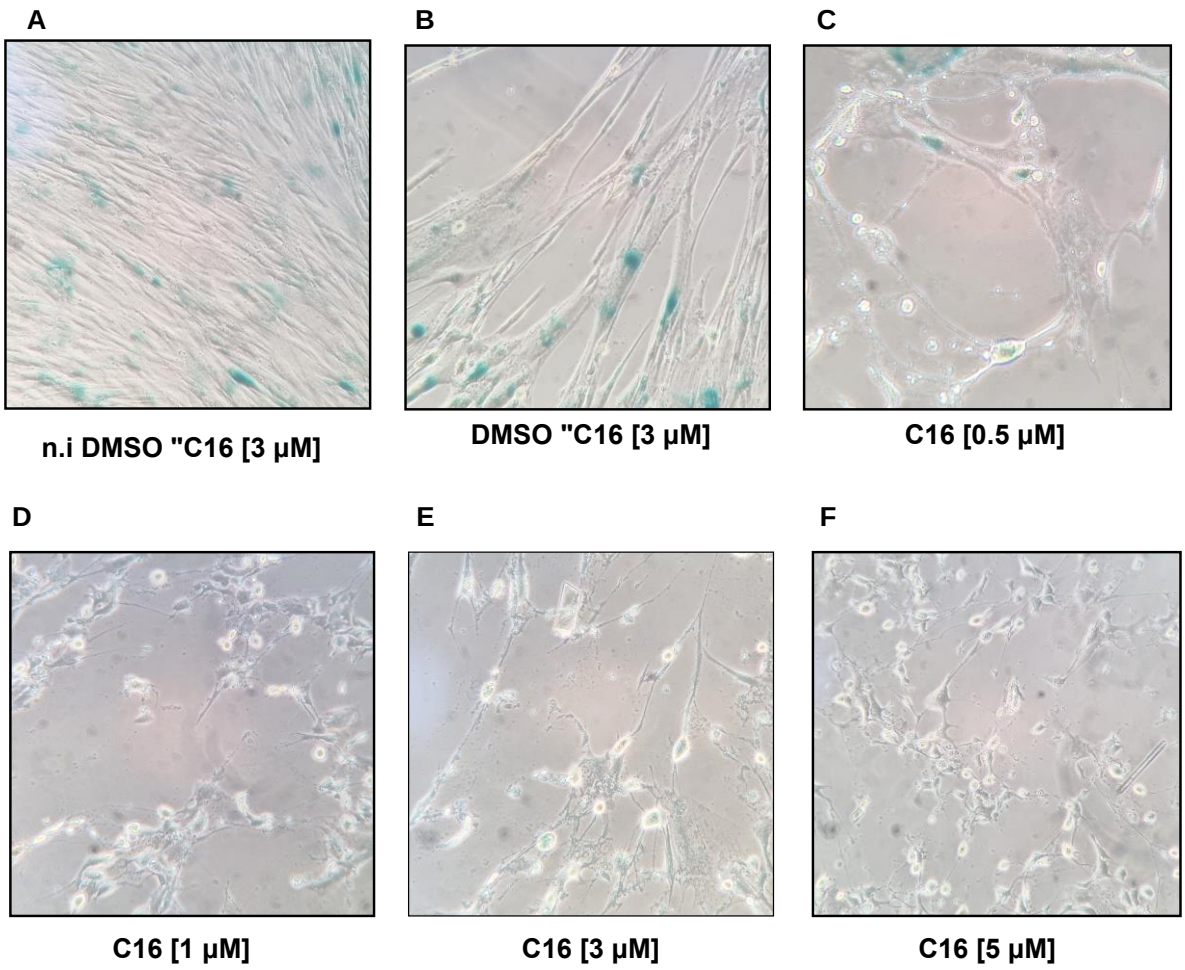

Figure 24: Microscopic images of senescence induced by RSV and prevented by PKR-IN-C16 senescence in WI-38 cells. WI-38 cells were treated with PKR inhibitor PKR-IN-C16 ([0.5 µM], [1 µM], [3 µM] or [5 µM]) 30 min prior to infection with RSV with multiplicity of infection (MOI) of 3 or incubated with medium (n.i.) for 72 h. Senescence was detected by senescence-associated β-galactosidase (SA-β-gal) assay and quantified as the amount of blue colored cells as a percentage of cells in total. (A) Light microscopic image of senescent cells stained blue using senescence-associated β-galactosidase (SA- β-gal) assay in non-infected (n.i) DMSO control for concentration of inhibitor (DMSO "C16 [3 µM]"). (B) RSV-infected DMSO control for concentration of inhibitor (DMSO "C16 [3 µM]"). Light microscopic image of senescent cells stained blue using SA-β-gal assay in cells treated with PKR inhibitor PKR-IN-C16 (C) [0.5 µM] (D) [1 µM] (E) [3 µM] (F) [5 µM]. The photographs were taken at total magnification 200x.

4 Discussion

In this study we examined the interaction between the unfolded protein response and viral infection. The UPR is crucial for managing ER stress caused by misfolded proteins, a condition often aggravated by viral infections. The unfolded protein response has been intimately linked to innate immunity. We also explored RSV-induced senescence in WI-38 cells. The PERK-eIF2α pathway has emerged to be more than a homeostatic cellular response to viral infection. We evaluated if the PERK-eIF2α pathway is activated by RSV infection and investigate whether the activation of PERK-eIF2α is dependent on STING or cGAS in WI-38 cells. Lastly, we investigated how RSV infection can be regulated through PERK and PKR inhibitors and how these inhibitors affect the expression of eIF2α.

4.1 cGAS and STING activation of PERK-eIF2α axis during RSV infection in WI-38 cells

Zhang et al. identified the previously unknown STING-PERK-eIF2α pathway, which regulates the cap-dependent mRNA translation. They state that STING is activated by binding to cGAMP which then binds to and directly activates the ER kinase PERK, triggering PERK's phosphorylation of eIF2α. This indicates a translation program that promotes inflammation and cell survival, operating independent from the unfolded protein response (30). The findings of the study "A non-canonical cGAS–STING–PERK pathway facilitates the translational program critical for senescence and organ fibrosis" served as the basis of our experiments.

We investigated if knockdown of cGAS or STING affected phosphorylation of PERK and eIF2α. Our findings demonstrate that KD of cGAS and STING does not affect phosphorylation of PERK or eIF2α, indicating that cGAS or STING is not required for induction of PERK-eIF2α. However, we did detect minimal decrease in phosphorylation of PKR in cGAS-STING-depleted cells relative to siAS treated cells, indicating that phosphorylation of PKR is connected to cGAS and STING to some extent. One possible reason for not obtaining the same results as Zhang et al. could be that they employed STING agonist 5,6-dimethylxanthenone-4-acetic acid (DMXAA) to induce stimulation of STING. STING might not have a significant effect on PERK at a lower stimuli or PERK might have been activated by other mechanisms than STING during STING KD. Another possible reason is that Zhang et al. used another cell type, not relevant for viral

infection. Our results suggests that cGAS-STING axis is not the most important signaling pathway during RSV infection and PERK-activation in WI-38 cells.

We found that KD of STING did not show reduction of CHOP mRNA. These results are consistant with the results of Zhang et al., where they investigated the STING-PERK pathway and demonstrated that ATF4-CHOP axis is activated by STING-PERK, but marginally. They suggested that ATF6-CHOP is activated by other UPR pathways to higher extent then through STING-PERK. Their data suggest that STING-PERK-eIF2α axis is spesific and independent of UPR or ER stress response (30). Additional research is necessary to establish a conclusive finding.

We did not observe a pronounced effect of cGAS-STING modulation in RSV infection, which may be related to lower contribution of cGAS-STING in the RSV response compared to other responses. Our results indicate that cGAS-STING axis is not important for phosphorylation of eIF2α or PERK in RSV-infected cell, however, it should be conducted more experiments to establish a conclusive finding. For future investigations it is interesting to further assess the effect of cGAS and STING KD in WI-38 cells infected with RSV. Additionllay, it would have been interesting to investigate the effect og knockout (KO) of cGAS and STING in a CRISPR-Cas9 KO cell line.

4.2 RSV induces UPR in WI-38 cells

Our results revealed that RSV infection induces ER stress and unfolded protein response in lung fibroblasts such as WI-38 cells. This was visualized by phosphorylation of eIF2α and PKR and through increased mRNA levels of UPR genes CHOP, IRE1 and XBP1 (Figure 25).

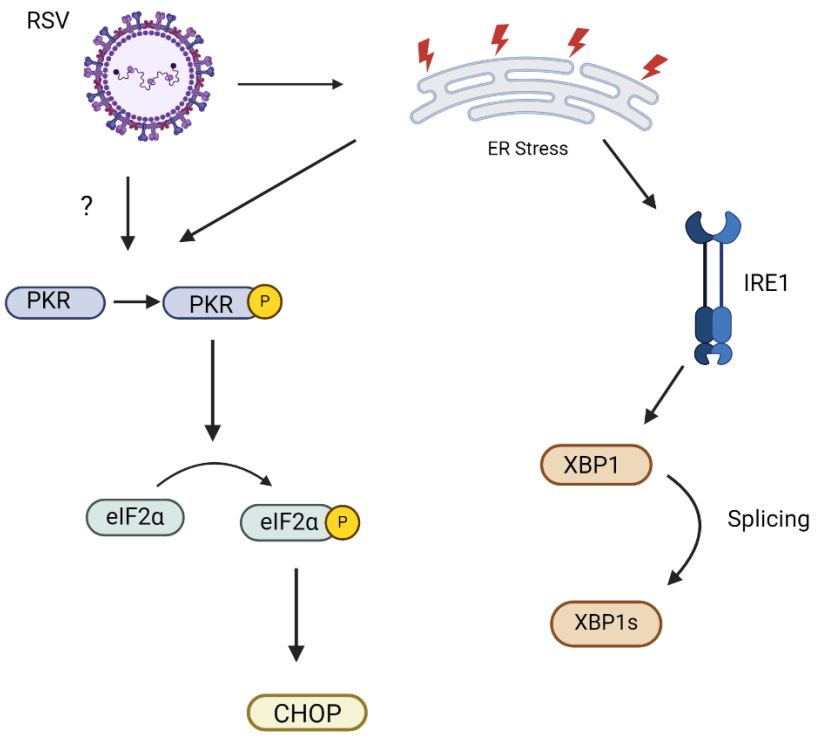

Figure 25: RSV infection induces ER stress and unfolded protein response (UPR) in the cell. RSV trigger autophosphorylation of PKR or induce ER stress which trigger activation of PKR. Activated PKR phosphorylates and activates eIF2α, which induces CHOP. RSV indicates ER stress in the cell and activation of UPR sensor IRE1, which in turn induces splicing of XBP1 and translation of spliced XBP1 (XBP1s). Created with BioRender.com

Our findings indicate that RSV infection activates the UPR, initially aiding the cell in managing the stress associated with viral protein production. In WI-38 cells, we found a corroborative increase in expression of the RSV fusion protein along with pPERK, peIF2α, pPKR. In addition, we observed enhanced expression of IRE1, XBP1 and CHOP, suggesting that viral protein induces UPR. Previous studies on ER stress and RSV in dendritic cells (DC) show similar results (64). Narayanan et al. show little up-regulation of IRE1 and PERK mRNA, and observed a significant upregulation of CHOP, suggesting that ER stress was increased during RSV infection in DCs (64). We revealed a more distinct increase in pPKR than in pPERK in WI-38 cells, supporting that PKR is activated by viral dsDNA and PERK is activated by ER stress (65). However, in HEp-2 cells we did not see the same increase in induction of pPERK and pPKR.

This revealed that activation of eIF2α through PERK and PKR after RSV infection might be dependent on cell types.

Some viruses can exploit the UPR to facilitate their replication. For example, enchancing protein folding capabilities might help the proper foldning and function of viral proteins (66). Some viruses can regulate CHOP expression to enhance its chance of survival (67). However, prolonged activation, indicated by increase in CHOP, might lead to cell death (46). CHOP seem to be involved in apoptosis and increased expression of CHOP mRNA suggest that the stress cannot be resolved, and the cell undergo programmed cell death as a protective mechanism (68). Apoptosis can be beneficial for viral replication, but it can also prompt the host cell to inhibit viral replication as a protective measure for uninfected cells. (68)

An upregulation of IRE1 and XBP1s mRNA, suggest that the cell not only activates the UPR sensor IRE1, but also increase its synthesis. IRE1 is a sensor for unfolded proteins and its activation leads to the splicing of XBP1 mRNA, which in turn enchanes the cell's ability to cope with unfolded proteins by increasing the capacity for protein foldning and degradation (69). This upregulation indicates a robust cellular attemt to enhance its capacity to manage ER stress by ensuring a higher availability of these critical sensors and transctiption factors. The increase in IRE1 and XBP1s mRNA implies that the cell is not only activating its existing IRE1 protein giving increase in XBP1 splicing and activation, but also upregulating the production of IRE1 itself, implying that there is a need for the more IRE1 activity. This could mean that the cell is ramping up its defence against the stress caused by viral proteins, improving its ability to manage ER stress over time. We did not observe a significant upregulation of ATF6, indicating that the UPR sensor was not activated by ER stress caused by RSV infection.

4.3 RSV induces senescence in WI-38 cells

Our results indicate that RSV induces scenescence in WI-38 cells. Senescence is a process of replicative aging or induced by e.g. oncogenes or virus in the cells (54, 70). Senescence happens after the cell reach an irreversible growth arrest and they change their functional state after a finite number of divisions. Senescent cells are often resistant to apoptosis and this causes an accumulation of senescent cells over time. (54)

UPR is activated in the host cell as a response to ER stress and to restore normal function in the cell. A previous study revealed evidence that prolonged activation of UPR, can lead to induction of cellular senescence as a respons mechanism to stress (62). Interestingly, a recent study revealed that SARS-CoV-2 induced cellular senescence (71). This study support our findings that prolonged activation of UPR due to RSV infection can induce senescence in WI-38 cells.

In addition to revealing that RSV induced senescence, we observed that the PKR inhibitor stronlgy inhibited RSV-mediated senescence induction. However, it was observed a reduction in cell confluency after treatment with PKR inhibitor. Indicating that the reduction in cell confluency gives less virus and reduced induction of senescence. Other studies have observed that KD of PKR caused cell death, and this gives reason to believe that inhibition of PKR might cause cell death and reduction in cell confluency (72).

Some studies have suggested that the cGAS-STING pathway is fundamental for senescence and apoptosis in human cells (30, 51) In the autoinflammatory disease SAVI, STING has been reported as a link to organ fibrosis and senescence (51). For future experiments, it would be interesting to further investigate the importance of cGAS-STING in induction of senescence.

4.4 Impacts of the PKR inhibitor PKR-IN-C16 on UPR and RSV replication dynamics in WI-38 cells

Our findings suggest that the PKR inhibitor decreased phosphorylation of PKR and eIF2α and expression of CHOP and XBP1s mRNA in WI-38 cells. This implies that the PKR inhibitor inhibits PKR-eIF2α-CHOP and IRE1-XBP1s axis. Inhibition of PKR might cause reduction in UPR activity shown by reduction in CHOP and XBP1s, and it might affect the ERs capasity to fold and stablize proteins correctly and lead to degradation of newly synthesized proteins. This would be interesting to investigate further.

Our findings revealed decrease in RSV fusion protein after treatment with the PKR inhibitor, however, RSV N-gene mRNA increased after the same treatment. One possible reason for increase in viral mRNA might be that the virus take advantage of the less stressed cellular machinery and makes the host cell produce more viral mRNA. A possible reason for decrease in RSV fusion protein, despite increase in viral mRN, might be that the inhibitor affected cell growth. Reduced cell growth might affect the prodction and release of viral protein. Previous

studies have revealed that the PKR inhibitor PKR-IN-C16 blocked tumor cell growth (73). Virus is dependent on cell growth for reproduction, and reduction in cell growth can therefore affect the replication of viral protein.

One important factor to mention is that there might have been conditions that compromised the cell viability, since it was observed a reduced cell confluency in after treatment with PKR inhibitor. Even though the PKR inhibitor increased viral mRNA, there might have been fever living cells in the lysate, giving false negative RSV fusion protein detection. In the furture, it would be interesting to investigate UPR respons in cell with siRNA-mediated KD of PKR.

5 Conclusion

This thesis has explored ER stress and UPR induced by RSV. Our findings confirm that RSV induces ER stress and activates specific branches of the UPR, notably through the IRE1-XBP1 and PKR-eIF2α axis. Our results also indicate that phosphorylation of eIF2α is mainly induced through PKR not PERK. Moreover, we revealed that RSV induced senescence in WI-38 cells and by treating cells with PKR inhibitor PKR-IN-C16, we observed a decrease in senescent cells after treatment. In addition, our results suggests that cGAS-STING is not the most important axis for activation of PERK in RSV-infected WI-38 cells.

Our results give insight into RSV-mediated UPR and senescence mechanisms in lung fibroblasts. As UPR and senescence are critical processes in fibroblasts and inflammation, our findings are relevant to RSV-mediated patogenesis. This insight is important for future research and development of strategies that could alleviate the effects of RSV, particularly in vulnerable populations such as infants. However, it is important to note that the results presented in this thesis are preliminary and require further research for validation and expansion.

In conclsion, this study offers valuable insight on the UPR, and senescence induced by RSV infection and the importance of PKR-eIF2α axis in response to RSV infection.

6 References

1. Jane Flint LWE, Vincent R. Racaniello, Glenn F. Rall, Anna Marie Skalka. Principles of Virology. 5 ed: John Wiley & Sons; 2020.
2. Hoenen T, Groseth A. Virus-Host Cell Interactions. Cells. 2022;11(5).
3. Weitnauer M, Mijošek V, Dalpke AH. Control of local immunity by airway epithelial cells. Mucosal Immunol. 2016;9(2):287-98.
4. Heinonen S, Rodriguez-Fernandez R, Diaz A, Oliva Rodriguez-Pastor S, Ramilo O, Mejias A. Infant Immune Response to Respiratory Viral Infections. Immunol Allergy Clin North Am. 2019;39(3):361-76.
5. Msemburi W, Karlinsky A, Knutson V, Aleshin-Guendel S, Chatterji S, Wakefield J. The WHO estimates of excess mortality associated with the COVID-19 pandemic. Nature. 2023;613(7942):130-7.
6. Zhang N, Wang L, Deng X, Liang R, Su M, He C, et al. Recent advances in the detection of respiratory virus infection in humans. J Med Virol. 2020;92(4):408-17.
7. Hodinka RL. Respiratory RNA Viruses. Microbiol Spectr. 2016;4(4).
8. Efstathiou C, Abidi SH, Harker J, Stevenson NJ. Revisiting respiratory syncytial virus's interaction with host immunity, towards novel therapeutics. Cell Mol Life Sci. 2020;77(24):5045-58.
9. Baker RE, Mahmud AS, Wagner CE, Yang W, Pitzer VE, Viboud C, et al. Epidemic dynamics of respiratory syncytial virus in current and future climates. Nat Commun. 2019;10(1):5512.
10. Guilliams M, Lambrecht BN, Hammad H. Division of labor between lung dendritic cells and macrophages in the defense against pulmonary infections. Mucosal Immunol. 2013;6(3):464-73.
11. Hirayama D, Iida T, Nakase H. The Phagocytic Function of Macrophage-Enforcing Innate Immunity and Tissue Homeostasis. Int J Mol Sci. 2017;19(1).
12. Mogensen TH. Pathogen recognition and inflammatory signaling in innate immune defenses. Clin Microbiol Rev. 2009;22(2):240-73, Table of Contents.
13. Marshall JS, Warrington R, Watson W, Kim HL. An introduction to immunology and immunopathology. Allergy Asthma Clin Immunol. 2018;14(Suppl 2):49.
14. Lang R, Li H, Luo X, Liu C, Zhang Y, Guo S, et al. Expression and mechanisms of interferon-stimulated genes in viral infection of the central nervous system (CNS) and neurological diseases. Front Immunol. 2022;13:1008072.
15. McNab F, Mayer-Barber K, Sher A, Wack A, O'Garra A. Type I interferons in infectious disease. Nat Rev Immunol. 2015;15(2):87-103.
16. Paolini R, Bernardini G, Molfetta R, Santoni A. NK cells and interferons. Cytokine Growth Factor Rev. 2015;26(2):113-20.
17. Mertowska P, Smolak K, Mertowski S, Grywalska E. Immunomodulatory Role of Interferons in Viral and Bacterial Infections. Int J Mol Sci. 2023;24(12).
18. Goubau D, Deddouche S, Reis e Sousa C. Cytosolic sensing of viruses. Immunity. 2013;38(5):855-69.
19. Ivashkiv LB, Donlin LT. Regulation of type I interferon responses. Nat Rev Immunol. 2014;14(1):36-49.
20. Piedimonte G, Perez MK. Respiratory syncytial virus infection and bronchiolitis. Pediatr Rev. 2014;35(12):519-30.
21. Nam HH, Ison MG. Respiratory syncytial virus infection in adults. Bmj. 2019;366:l5021.
22. Azzari C, Baraldi E, Bonanni P, Bozzola E, Coscia A, Lanari M, et al. Epidemiology and prevention of respiratory syncytial virus infections in children in Italy. Ital J Pediatr. 2021;47(1):198.
23. Shang Z, Tan S, Ma D. Respiratory syncytial virus: from pathogenesis to potential therapeutic strategies. Int J Biol Sci. 2021;17(14):4073-91.
24. Christiaansen AF, Syed MA, Ten Eyck PP, Hartwig SM, Durairaj L, Kamath SS, Varga SM. Altered Treg and cytokine responses in RSV-infected infants. Pediatr Res. 2016;80(5):702-9.
25. Griffiths C, Drews SJ, Marchant DJ. Respiratory Syncytial Virus: Infection, Detection, and New Options for Prevention and Treatment. Clin Microbiol Rev. 2017;30(1):277-319.

26. Norlander AE, Peebles RS, Jr. Innate Type 2 Responses to Respiratory Syncytial Virus Infection. Viruses. 2020;12(5).
27. Villenave R, Shields MD, Power UF. Respiratory syncytial virus interaction with human airway epithelium. Trends Microbiol. 2013;21(5):238-44.
28. Bergeron HC, Tripp RA. Immunopathology of RSV: An Updated Review. Viruses. 2021;13(12).
29. Van Royen T, Rossey I, Sedeyn K, Schepens B, Saelens X. How RSV Proteins Join Forces to Overcome the Host Innate Immune Response. Viruses. 2022;14(2).
30. Zhang D, Liu Y, Zhu Y, Zhang Q, Guan H, Liu S, et al. A non-canonical cGAS-STING-PERK pathway facilitates the translational program critical for senescence and organ fibrosis. Nat Cell Biol. 2022;24(5):766-82.
31. Ou L, Zhang A, Cheng Y, Chen Y. The cGAS-STING Pathway: A Promising Immunotherapy Target. Front Immunol. 2021;12:795048.
32. Amurri L, Horvat B, Iampietro M. Interplay between RNA viruses and cGAS/STING axis in innate immunity. Front Cell Infect Microbiol. 2023;13:1172739.
33. Hopfner KP, Hornung V. Molecular mechanisms and cellular functions of cGAS-STING signalling. Nat Rev Mol Cell Biol. 2020;21(9):501-21.
34. Decout A, Katz JD, Venkatraman S, Ablasser A. The cGAS-STING pathway as a therapeutic target in inflammatory diseases. Nat Rev Immunol. 2021;21(9):548-69.
35. Xiang C, Wang Y, Zhang H, Han F. The role of endoplasmic reticulum stress in neurodegenerative disease. Apoptosis. 2017;22(1):1-26.
36. Stone S, Lin W. The unfolded protein response in multiple sclerosis. Front Neurosci. 2015;9:264.
37. Rozpedek W, Pytel D, Mucha B, Leszczynska H, Diehl JA, Majsterek I. The Role of the PERK/eIF2α/ATF4/CHOP Signaling Pathway in Tumor Progression During Endoplasmic Reticulum Stress. Curr Mol Med. 2016;16(6):533-44.
38. Shacham T, Patel C, Lederkremer GZ. PERK Pathway and Neurodegenerative Disease: To Inhibit or to Activate? Biomolecules. 2021;11(3).
39. Walczak A, Gradzik K, Kabzinski J, Przybylowska-Sygut K, Majsterek I. The Role of the ER-Induced UPR Pathway and the Efficacy of Its Inhibitors and Inducers in the Inhibition of Tumor Progression. Oxid Med Cell Longev. 2019;2019:5729710.
40. Hazari Y, Hetz C. A chosen STING with a PERKy trail. Nat Cell Biol. 2022;24(5):602-4.
41. Inoue T, Tsai B. How viruses use the endoplasmic reticulum for entry, replication, and assembly. Cold Spring Harb Perspect Biol. 2013;5(1):a013250.
42. Di Conza G, Ho PC. ER Stress Responses: An Emerging Modulator for Innate Immunity. Cells. 2020;9(3).
43. Lee ES, Yoon CH, Kim YS, Bae YS. The double-strand RNA-dependent protein kinase PKR plays a significant role in a sustained ER stress-induced apoptosis. FEBS Lett. 2007;581(22):4325-32.
44. Liu Y, Wang M, Cheng A, Yang Q, Wu Y, Jia R, et al. The role of host eIF2α in viral infection. Virol J. 2020;17(1):112.
45. Jaud M, Philippe C, Di Bella D, Tang W, Pyronnet S, Laurell H, et al. Translational Regulations in Response to Endoplasmic Reticulum Stress in Cancers. Cells. 2020;9(3).
46. Ghemrawi R, Khair M. Endoplasmic Reticulum Stress and Unfolded Protein Response in Neurodegenerative Diseases. Int J Mol Sci. 2020;21(17).
47. Hetz C. The unfolded protein response: controlling cell fate decisions under ER stress and beyond. Nat Rev Mol Cell Biol. 2012;13(2):89-102.
48. Walter P, Ron D. The unfolded protein response: from stress pathway to homeostatic regulation. Science. 2011;334(6059):1081-6.
49. Kumari R, Jat P. Mechanisms of Cellular Senescence: Cell Cycle Arrest and Senescence Associated Secretory Phenotype. Front Cell Dev Biol. 2021;9:645593.
50. Yu Q, Katlinskaya YV, Carbone CJ, Zhao B, Katlinski KV, Zheng H, et al. DNA-damage-induced type I interferon promotes senescence and inhibits stem cell function. Cell Rep. 2015;11(5):785-97.

51. de Cevins C, Delage L, Batignes M, Riller Q, Luka M, Remaury A, et al. Single-cell RNA-sequencing of PBMCs from SAVI patients reveals disease-associated monocytes with elevated integrated stress response. Cell Rep Med. 2023;4(12):101333.
52. Schmitt CA, Tchkonia T, Niedernhofer LJ, Robbins PD, Kirkland JL, Lee S. COVID-19 and cellular senescence. Nat Rev Immunol. 2023;23(4):251-63.
53. Kurz DJ, Decary S, Hong Y, Erusalimsky JD. Senescence-associated (beta)-galactosidase reflects an increase in lysosomal mass during replicative ageing of human endothelial cells. J Cell Sci. 2000;113 (Pt 20):3613-22.
54. Valieva Y, Ivanova E, Fayzullin A, Kurkov A, Igrunkova A. Senescence-Associated β-Galactosidase Detection in Pathology. Diagnostics (Basel). 2022;12(10).
55. Martínez I, García-Carpizo V, Guijarro T, García-Gomez A, Navarro D, Aranda A, Zambrano A. Induction of DNA double-strand breaks and cellular senescence by human respiratory syncytial virus. Virulence. 2016;7(4):427-42.
56. Chuprin A, Gal H, Biron-Shental T, Biran A, Amiel A, Rozenblatt S, Krizhanovsky V. Cell fusion induced by ERVWE1 or measles virus causes cellular senescence. Genes Dev. 2013;27(21):2356-66.
57. ATCC. WI-38 [
58. Hu B, Zhong L, Weng Y, Peng L, Huang Y, Zhao Y, Liang XJ. Therapeutic siRNA: state of the art. Signal Transduct Target Ther. 2020;5(1):101.
59. Rajan A, Piedra FA, Aideyan L, McBride T, Robertson M, Johnson HL, et al. Multiple Respiratory Syncytial Virus (RSV) Strains Infecting HEp-2 and A549 Cells Reveal Cell Line-Dependent Differences in Resistance to RSV Infection. J Virol. 2022;96(7):e0190421.
60. Donnelly N, Gorman AM, Gupta S, Samali A. The eIF2α kinases: their structures and functions. Cell Mol Life Sci. 2013;70(19):3493-511.
61. Hosakote YM, Brasier AR, Casola A, Garofalo RP, Kurosky A. Respiratory Syncytial Virus Infection Triggers Epithelial HMGB1 Release as a Damage-Associated Molecular Pattern Promoting a Monocytic Inflammatory Response. J Virol. 2016;90(21):9618-31.
62. Abbadie C, Pluquet O. Unfolded Protein Response (UPR) Controls Major Senescence Hallmarks. Trends Biochem Sci. 2020;45(5):371-4.
63. Torrano J, Al Emran A, Hammerlindl H, Schaider H. Emerging roles of H3K9me3, SETDB1 and SETDB2 in therapy-induced cellular reprogramming. Clin Epigenetics. 2019;11(1):43.
64. Narayanan S, Elesela S, Rasky AJ, Morris SH, Kumar S, Lombard D, Lukacs NW. ER stress protein PERK promotes inappropriate innate immune responses and pathogenesis during RSV infection. J Leukoc Biol. 2022;111(2):379-89.
65. Dabo S, Meurs EF. dsRNA-dependent protein kinase PKR and its role in stress, signaling and HCV infection. Viruses. 2012;4(11):2598-635.
66. Chen YJ, Bagchi P, Tsai B. ER functions are exploited by viruses to support distinct stages of their life cycle. Biochem Soc Trans. 2020;48(5):2173-84.
67. Turpin J, El-Safadi D, Lebeau G, Frumence E, Desprès P, Viranaïcken W, Krejbich-Trotot P. CHOP Pro-Apoptotic Transcriptional Program in Response to ER Stress Is Hacked by Zika Virus. Int J Mol Sci. 2021;22(7).
68. Hu H, Tian M, Ding C, Yu S. The C/EBP Homologous Protein (CHOP) Transcription Factor Functions in Endoplasmic Reticulum Stress-Induced Apoptosis and Microbial Infection. Front Immunol. 2018;9:3083.
69. Siwecka N, Rozpędek-Kamińska W, Wawrzynkiewicz A, Pytel D, Diehl JA, Majsterek I. The Structure, Activation and Signaling of IRE1 and Its Role in Determining Cell Fate. Biomedicines. 2021;9(2).
70. Seoane R, Vidal S, Bouzaher YH, El Motiam A, Rivas C. The Interaction of Viruses with the Cellular Senescence Response. Biology (Basel). 2020;9(12).
71. Gioia U, Tavella S, Martínez-Orellana P, Cicio G, Colliva A, Ceccon M, et al. SARS-CoV-2 infection induces DNA damage, through CHK1 degradation and impaired 53BP1 recruitment, and cellular senescence. Nat Cell Biol. 2023;25(4):550-64.

72. Pataer A, Swisher SG, Roth JA, Logothetis CJ, Corn PG. Inhibition of RNA-dependent protein kinase (PKR) leads to cancer cell death and increases chemosensitivity. Cancer Biol Ther. 2009;8(3):245-52.
73. Watanabe T, Ninomiya H, Saitou T, Takanezawa S, Yamamoto S, Imai Y, et al. Therapeutic effects of the PKR inhibitor C16 suppressing tumor proliferation and angiogenesis in hepatocellular carcinoma in vitro and in vivo. Sci Rep. 2020;10(1):5133.

7 Appendix

S.1 Knockdown (KD) efficiency (%) of cGAS and STING

Calculated KD-efficiency (%) of cGAS and STING in non-infected and RSV-infected WI-38 cells. A % efficiency over 80% was considered good.

Table 1: Knockdown (KD) efficiency (%) of cGAS and STING in WI-38 cells. WI-38 cells were reverse transfected with cGAS or STING with a concentration of 10nM for 24 h prior to RSV infection with a multiplicity of infection (MOI) of 3 for 48 h. KD efficiency was calculated by expression of cGAS and STING mRNA in sicGAS and STING transfected samples relative to control siRNA siAllstar (siAS). The relative expression was converted to % and subtracted from 100%.

	Non-infected	RSV-infected
sicGAS	82%	89%
siSTING	84%	87%

S.2 Primer sequences and antibodies

Primer sequences for different genes used to analyze mRNA expression by RT-qPCR are listed in Table 2. Primary antibodies used to analyze protein expression by Western blot are listed in Table 3 and secondary antibodies are listed in Table 4.

Table 2: Primer sequences for different genes used for analysis of mRNA expression by RT-qPCR.

Gene	Forward (5'-3')	Reverse (5'-3')
RSV N	CYAARTTAGCAGCAGGGRAYAG	CTGTTRGCTATRTCCTTKGGT
CHOP	GGCAGCGACAGAGCCAAAAT	GCTTTCAGGTGTGGTGATGATGA
IFN-β	GCCGCATTGACCATCTATGAGA	GAGATCTTCAGTTTCGGAGGTAAC
hXBP1s	GCTGAGTCCGCAGCAGG	CTCTGGGGAAGGGCATTTGA
hXBP1us	AAGCCAAGGGGAATGAAGTGA	GCCAGAATCCATGGGGAGATG
hIRE1	TGTGTCAACGCTGGATGGAA	TCCACATGTGTTGGGACCTG
hATF6	CCGTATTCTTCAGGGTGCTCT	AGCTCACTCCCTGAGTTCCTG
cGAS	ACATGGCGGCTATCCTTCTCT	GGGTTCTGGGTACATACGTGAAA
STING	TCAAGGATCGGGTTTACAGC	TGGCAAACAAAGTCTGCAAG

Table 3: Primary antibodies used in Western blot, with manufacturer, dilution and species.

Antibody	Manufacturer (Catalog number)	Dilution	Species
RSV F	Novus Biologicals (#NB110-37246)	1:500	Mouse
peIF2α (S51)	Cell Signaling Technology (#9721)	1:1000	Rabbit
pPERK (Thr982)	Invitrogen (#PA5-40294)	1:2000	Rabbit
pPKR (Thr 446/451)	Cell Signaling Technology (#3071)	1:500	Rabbit
PKR	Cell Signaling Technology (#3072)	1:500	Rabbit
cGAS	Cell Signaling Technology (#15102)	1:1000	Rabbit IgG
pSTING (Ser366)	Cell Signaling Technology (#50907)	1:1000	Rabbit IgG
STING	Cell Signaling Technology (#13647)	1:1000	Rabbit IgG
H3k9me3	Diagenode (#15410193)	1:1000	Rabbit
GADPH	Cell Signaling Technology (#5174)	1:10 000	Rabbit IgG

Table 4*:* Secondary antibodies used in Western Blot, with manufacturer, dilution, and immunogen.

Antibody	Manufacturer (Catalog number)	Dilution	Immunogen
IRDye GAR 800CW	LI-COR Biosciences (#926-32211)	1:5000	Rabbit IgG
IRDye GAR 680RD	LI-COR Biosciences (#926-68071)	1:20 000	Rabbit IgG
IRDye GAM 800CW	LI-COR Biosciences (#926-32210)	1:5000	Mouse IgG

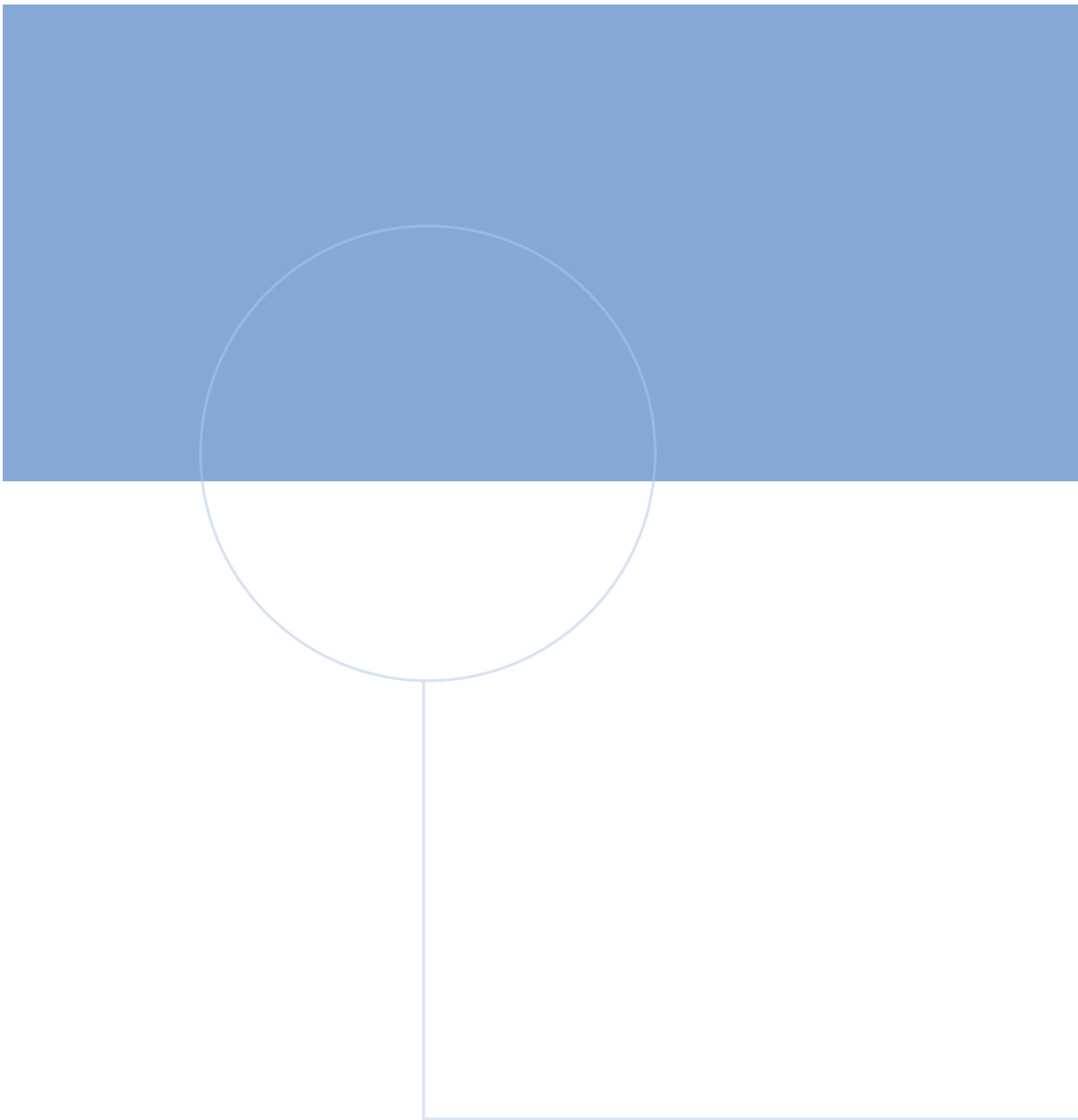

NTNU

Norwegian University of
Science and Technology